Neurobiology of Disease 145 (2020) 105051

Contents lists available at ScienceDirect

Neurobiology of Disease

journal homepage: www.elsevier.com/locate/ynbdi

Chronic stress induces formation of stress granules and pathological TDP-43 aggregates in human ALS fibroblasts and iPSC-motoneurons

Antonia Ratti[a,b], Valentina Gumina[a], Paola Lenzi[c], Patrizia Bossolasco[a], Federica Fulceri[d], Clara Volpe[a,b], Donatella Bardelli[a,e], Francesca Pregnolato[f], AnnaMaria Maraschi[a], Francesco Fornai[c,g], Vincenzo Silani[a,e,h,1], Claudia Colombrita[a,*,1]

[a] Istituto Auxologico Italiano, IRCCS, Department of Neurology-Stroke Unit and Laboratory of Neuroscience, Piazzale Brescia 20, 20149 Milan, Italy
[b] Department of Medical Biotechnology and Translational Medicine, Università degli Studi di Milano, Via Fratelli Cervi 93, 20090 Segrate, Milan, Italy
[c] Department of Translational Research and New Technologies in Medicine and Surgery, University of Pisa, via Roma 55, 56126 Pisa, Italy
[d] Department of Clinical and Experimental Medicine, University of Pisa, Via Roma 55, Pisa 56126, Italy
[e] "Aldo Ravelli" Center for Neurotechnology and Experimental Brain Therapeutics, Università degli Studi di Milano, Via A. di Rudinì 8, 20142 Milan, Italy
[f] Istituto Auxologico Italiano, IRCCS, Immunorheumatology Research Laboratory, Via Zucchi 18, 20095 Cusano Milanino, Milan, Italy
[g] I.R.C.C.S. Neuromed, via Atinense 18, 86077 Pozzilli (IS), Italy
[h] Department of Pathophysiology and Transplantation, "Dino Ferrari" Center, Università degli Studi di Milano, Via F. Sforza 35, 20122 Milan, Italy

ARTICLE INFO

Keywords:
Stress granules
Chronic stress
ALS
TDP-43
Pathological aggregates
Fibroblast
iPSC-derived motoneuron

ABSTRACT

Amyotrophic lateral sclerosis (ALS) and frontotemporal dementia (FTD) are fatal neurodegenerative diseases characterized by the presence of neuropathological aggregates of phosphorylated TDP-43 (P-TDP-43) protein. The RNA-binding protein TDP-43 participates also to cell stress response by forming stress granules (SG) in the cytoplasm to temporarily arrest translation. The hypothesis that TDP-43 pathology directly arises from SG has been proposed but is still under debate because only sub-lethal stress conditions have been tested experimentally so far. In this study we reproduced a mild and chronic oxidative stress by sodium arsenite to better mimic the persistent and subtle alterations occurring during the neurodegenerative process in primary fibroblasts and induced pluripotent stem cell-derived motoneurons (iPSC-MN) from ALS patients carrying mutations in *TARDBP* and *C9ORF72* genes. We found that not only the acute sub-lethal stress usually used in literature, but also the chronic oxidative insult was able to induce SG formation in both primary fibroblasts and iPSC-MN. We also observed the recruitment of TDP-43 into SG only upon chronic stress in association to the formation of distinct cytoplasmic P-TDP-43 aggregates and a significant increase of the autophagy marker p62. A quantitative analysis revealed differences in both the number of cells forming SG in mutant ALS and healthy control fibroblasts, suggesting a specific genetic contribution to cell stress response, and in SG size, suggesting a different composition of these cytoplasmic foci in the two stress conditions. Upon removal of arsenite, the recovery from chronic stress was complete for SG and P-TDP-43 aggregates at 72 h with the exception of p62, which was reduced but still persistent, supporting the hypothesis that autophagy impairment may drive pathological TDP-43 aggregates formation. The gene-specific differences observed in fibroblasts in response to oxidative stress were not present in iPSC-MN, which showed a similar formation of SG and P-TDP-43 aggregates regardless their genotype. Our results show that SG and P-TDP-43 aggregates may be recapitulated in patient-derived neuronal and non-neuronal cells exposed to prolonged oxidative stress, which may be therefore exploited to study TDP-43 pathology and to develop individualized therapeutic strategies for ALS/FTD.

Abbreviations: ALS, amyotrophic lateral sclerosis; ARS, sodium arsenite; FTD, frontotemporal dementia; iPSC-MN, iPSC-derived motoneurons; LCD, low-complexity domain; LLPS, liquid-liquid phase separation; mC9ORF72, mutant C9ORF72; mTDP-43, mutant TARDBP p.A382T; P-TDP-43, phosphorylated TDP-43; RBP, RNA-binding protein; SG, stress granules; TEM, Transmission electron microscopy

* Corresponding author.
E-mail addresses: antonia.ratti@unimi.it (A. Ratti), paola.lenzi@med.unipi.it (P. Lenzi), federica.fulceri@unipi.it (F. Fulceri), clara.volpe@unimi.it (C. Volpe), francesco.fornai@neuromed.it (F. Fornai), vincenzo@silani.com (V. Silani), c.colombrita@auxologico.it (C. Colombrita).
[1] These authors contributed equally to this work

https://doi.org/10.1016/j.nbd.2020.105051
Received 11 April 2020; Received in revised form 18 July 2020; Accepted 13 August 2020
Available online 20 August 2020

1. Introduction

Abnormal cytoplasmic aggregates of TDP-43 protein represent the neuropathological hallmark of TDP-43 proteinopathies including amyotrophic lateral sclerosis (ALS) and frontotemporal dementia (FTD), two fatal neurodegenerative diseases which share some clinical and genetic features (Abramzon et al., 2020; Ling et al., 2013). Pathological inclusions of phosphorylated and ubiquitinated TDP-43 protein are present in about 97% of autoptic brains from familial and sporadic ALS and in about 45% of FTD patients (Arai et al., 2006; Ling et al., 2013; Neumann et al., 2006). TDP-43 is an ubiquitously expressed RNA-binding protein (RBP) that contains a C-terminal low-complexity domain (LCD), rich in glycine, glutamine and asparagine residues and important for protein-protein interaction (Ratti and Buratti, 2016). Although it localizes mainly in the nucleus regulating splicing, TDP-43 is able to shuttle between the nucleus and the cytoplasm (Ratti and Buratti, 2016) where, under stress conditions, is recruited into stress granules (SG), as demonstrated in different cellular models (Birsa et al., 2019; Colombrita et al., 2009). SG are reversible and dynamic membrane-less cytoplasmic protein/RNA complexes which form in response to environmental stress as a protective mechanism to temporarily arrest translation and favour only the synthesis of cytoprotective proteins (Kedersha and Anderson, 2002).

From a biophysical point of view, assembly of SG has been shown to occur *via* a liquid-liquid phase separation (LLPS) process through which soluble cytoplasmic protein/RNA complexes condensate into dynamic liquid droplets (Hyman et al., 2014; Wippich et al., 2013) by weak and reversible interactions of the LCDs present in several RBPs, including TDP-43 (Harrison and Shorter, 2017). After stress removal, SG usually disassemble through a chaperone-mediated mechanism, while a small fraction of aberrant SG, which accumulates defective ribosomal products, fails to completely disassemble being then degraded by autophagy (Chitiprolu et al., 2018; Ganassi et al., 2016; Monahan et al., 2016). Some evidence also suggest the involvement of the proteasome system in SG removal so that the complex interaction among chaperones, autophagy, and proteasome system plays an important role in SG dynamics (Cascella et al., 2017; Mahboubi and Stochaj, 2017; Monahan et al., 2016).

In the last decade, several ALS-associated proteins have been identified as components of SG other than TDP-43, and SG formation has been hypothesized to trigger the neurodegenerative process through sequestration of important RBPs and factors and as an early precursor of TDP-43 pathological aggregates (Aulas and Velde, 2015; Mahboubi and Stochaj, 2017). In particular, in condition of persistent oxidative stress in the course of neurodegeneration, SG are supposed to fail in their proper disassembly and to progressively turn into insoluble and irreversible aggregates, thus disrupting neuronal homeostasis and eventually interfering with the protein quality control system (Monahan et al., 2016).

However, controversial reports fail to show a clear co-localization of SG markers with TDP-43-positive pathological inclusions in the brain and spinal cord autoptic tissues obtained from ALS/FTD patients (Bentmann et al., 2012; Colombrita et al., 2009; Dormann et al., 2010; Liu-Yesucevitz et al., 2010; McGurk et al., 2014; Volkening et al., 2009). Nonetheless, recent findings indicate that, even if they appear as distinct entities, a mechanistic link between SG and pathological TDP-43 inclusions may occur (Fang et al., 2019; Gasset-Rosa et al., 2019; Mann et al., 2019; McGurk et al., 2018). A missing point in this proposed pathomechanism is the evidence that TDP-43 aggregates directly arise from SG because the short-acting and extreme insults used so far to induce SG formation are indeed quite far from reproducing the persistent and subtle alterations occurring during neurodegeneration.

To address this issue, in this study we reproduced a persistent and mild oxidative stress by treating ALS patient-derived cells, including fibroblasts and induced pluripotent stem cell-derived motoneurons (iPSC-MN), with sodium arsenite and investigated their response to stress and SG formation in this experimental condition which better mimics the neurodegenerative process.

2. Materials and methods

2.1. Primary fibroblast cultures

Primary fibroblasts were isolated from skin biopsies of unrelated ALS patients carrying mutations in *TARDBP* (p.A382T, mTDP-43, $n = 3$) and *C9ORF72* (mC9ORF72, $n = 3$) genes and of sex- and age-matched healthy controls ($n = 3$; one sample was obtained from the Telethon Biobank), after informed consent and according to guidelines approved by the local ethics committee. Clinical data of ALS patients are reported in Supplementary Table S1 and already described in Onesto et al., 2016. Fibroblasts were maintained in DMEM supplemented with 1 mM sodium pyruvate (Thermo Fisher Scientific, Waltham, MA), 20% fetal bovine serum (FBS), 2,5 μg/ml amphotericin B, 100 units/ml penicillin and 100 μg/ml streptomycin (Sigma-Aldrich, St. Louis, MO) in 5% CO_2 incubator at 37 °C. Fibroblasts were used in the experiments for no more than 12 passages.

2.2. iPSC-derived motoneurons

iPSC lines from 1 healthy control, 1 mutant *TARDBP* p.A382T and 1 mutant *C9ORF72* ALS patient were obtained by reprogramming fibroblasts (Supplementary Table S1) with CytoTune-iPS 2.0 Sendai Reprogramming Kit (Thermo Fisher Scientific, Waltham, MA) and differentiated into motoneurons (iPSC-MN), as previously described (Bardelli et al., 2020; Bossolasco et al., 2018). Briefly, iPSCs were grown in suspension in low adhesion cell culture dishes and embryoid bodies (EBs) formation was induced in 17 days by using different culture media supplemented with appropriate growth factors (Bardelli et al., 2020; Bossolasco et al., 2018). EBs were then dissociated and 15,000 cells/well were plated on poly-D-Lysine/laminin (Thermo Fisher Scientific) -coated glass coverslips in 24-well plates. After additional 10 days differentiation, the obtained iPSC-MN were treated with sodium arsenite (see below). Motoneuronal differentiation efficiency was characterized by immunofluorescence assay with the neuronal cytoskeleton markers βIII-Tubulin (1:500, Abcam, Cambridge, UK) and phosphorylated neurofilaments (SMI-312; 1:1000, Covance, Princetown, NJ), and the motoneuronal marker HB9 (1:200, DSHB, Iowa city, IA).

2.3. Arsenite treatment

For acute oxidative stress treatment, fibroblasts were exposed to 0.5 mM sodium arsenite (ARS, Merck, Darmstadt, Germany) for 30 and 60 min. As no substantial differences were appreciated at 60 min in comparison with 30 min-treatment, we used 0.5 mM ARS for 30 min for all the following acute stress experiments. As regards chronic stress conditions, different concentrations of ARS were tested in fibroblasts for several timepoints, as follows: 5 μM for 24–48–54-72-96 h and 8 days; 15 μM for 6–15–20-30-48 h and 50 μM for 6–16 h. Rescue experiments were performed by restoring normal cell growth conditions for 2 h after acute ARS treatment and for 24–48-72 h after chronic ARS treatment. iPSC-MN were exposed to 0.5 mM ARS for 60 min, while for chronic stress they were treated with the following conditions: 10-15 μM ARS for 16–24-48 h and 1-5 μM for 48–72-96 h and 7 days.

2.4. Cell viability assay

Fibroblasts (50.000 cells/well) were plated in duplicate for each patient's sample in 24-well dishes, 24 h before the experiment. After treatment with 0.5 mM ARS for 30 min and 15 μM ARS for 30 h, both medium and adherent fibroblasts were collected to determine viable/non-viable cells. After centrifugation at 1000 rpm for 10 min,

supernatant was discarded, and pellet was resuspended in 500 μl medium. Cells were diluted 1:2 with trypan blue stain 0.4% (Logos Biosystems, South Korea) to label non-viable cells and cell viability was evaluated by using the Luna-II automated cell counter (Logos Biosystems) with a custom cell-specific counting protocol.

2.5. Immunofluorescence

Cells were fixed in 4% paraformaldehyde solution (Santa Cruz Biotechnology, Dallas, TX) for 20 min at room temperature (RT), permeabilized with cold methanol for 3 min and 0.3% Triton X-100 in phosphate buffered saline (PBS, pH 7.4, Thermo Fisher Scientific) and blocked with 10% normal goat serum (NGS, Thermo Fisher Scientific) in PBS. Incubation with the primary antibodies anti-TDP-43 (1:500, Proteintech, Auckland, New Zealand), anti-TIAR (mouse 1:100, BD transduction Laboratories, Franklin Lakes, NJ; rabbit 1:300, Cell Signaling, Danvers, Massachusetts), anti-p62 (1:500, Sigma-Aldrich), anti-phosphoTDP-43 (Ser 409/410 1:200, Cosmo Bio, Carlsbad, CA) was performed in blocking solution for 1.30 h at 37 °C. The fluorescent-tagged secondary antibodies Alexa Fluor 488 and Alexa Fluor 555 (1:500, Thermo Fisher Scientific) were used for detection. As negative control, primary antibody was replaced by blocking solution. Nuclei were stained with 4′6-diamidino-2-phenylindole (DAPI) (Roche, Basilea, Switzerland) and slides were mounted with Fluorsave reagent (Merck). Confocal images were acquired with the Eclipse Ti inverted microscope (Nikon Eclipse C1, Minato, Japan) as *Z*-stacks (0.2 μm step size) with a 60× magnification.

2.6. Quantitative analyses of SG

Quantification of cells forming SG and of granules number and size was performed using the ImageJ software (NIH), as previously reported (Ross Buchan et al., 2010). SG were identified by TIAR marker immunostaining and at least 60 cells per sample were analyzed. On the basis of previous literature data (Anderson, 2009; Aulas et al., 2015; Orrù et al., 2016), cytoplasmic granules were divided into three arbitrary size categories (0.1- $<$ 0.75 μm^2, 0.75-5 μm^2 and $>$ 5 μm^2) and cells were scored as SG-positive when they presented at least two cytoplasmic foci $\geq 0.75 \mu m^2$. Cell counting was performed in double-blind on 60× magnification images. Experiments were conducted on 3 different samples per group of fibroblasts (n = 3 CTRLs, n = 3 mTDP-43, n = 3 mC9ORF72) and for each cell sample the experiment was repeated 2–5 times. Cell counting in iPSC-MN was conducted on 1 sample per group (CTRL, mTDP-43, mC9ORF72) and repeated for two different motoneuronal differentiations.

2.7. Colocalization image analysis

Quantification of TDP-43 and TIAR colocalization signals in SG was obtained using coloc2 plugin of the Fiji version (http://fiji.sc) of ImageJ software. Pearson's correlation coefficient (r) was calculated from five randomly selected cells from each sample group of fibroblasts and co-localization was defined as “strong” when r values were $>$ 0.7 (Dunn et al., 2011).

2.8. Transmission electron microscopy (TEM)

Fibroblasts (4×10^6 cells) were incubated with the fixing solution glutaraldehyde 3% (Sigma-Aldrich) in PBS pH 7.4 for 90 min at 4 °C. Cells were then collected by centrifugation at 10,000 rpm for 10 min at 4 °C to form a buffy coat of cells, washed with PBS and post-fixed in 1% OsO_4 for 1 h at 4 °C to prevent the formation of membranous artifacts, which may mimic autophagic vacuoles in TEM analyses (Swanlund et al., 2010). Samples were dehydrated in ethanol and finally embedded in epoxy resin as previously described (Lenzi et al., 2016), to maintain the finest cell ultrastructure and to preserve epitopes for immunocytochemistry. Ultrathin sections (40–50 nm) were used for post-embedding immune-electron microscopy (Lenzi et al., 2016). Briefly, sections were collected on nickel grids and incubated in aqueous saturated $NaIO_4$ for 30 min at RT. Grids were incubated in blocking buffer (10% goat serum and 0.2% saponin in PBS) for 20 min at RT and then overnight at 4 °C in a humidified chamber with the following antibodies: LC3 (1:50, Abcam), p62 (1:20, Sigma-Aldrich), TIAR (1:20, BD transduction Laboratories) and phosphoTDP-43 (Ser 409/410) (1:20, Cosmo Bio). Grids were then washed in cold PBS before applying the gold-conjugated secondary antibodies (10 or 20 nm gold particles, BB International, Treviso, Italy), diluted (1:20) in blocking buffer for 1 h at RT. Sections were examined at Jeol JEM SX 100 electron microscope (Jeol, Tokyo, Japan) at 8.000× magnification. Control sections were obtained by omitting the primary antibody and by incubating with the secondary antibody only.

2.9. Quantitative analysis of TEM data

The count of 10 nm and 20 nm immune-gold particles was carried out by electron microscopy at 8.000× magnification. We scored as ATG-like vacuoles both double or multiple membranes (autophagosomes-like) containing cytoplasmic material and electron-dense membranous structures (Lenzi et al., 2016). A total number of 30 cells per experimental group was analyzed in non-serial sections of each grid.

2.10. Statistical analysis

Statistical analysis was conducted with PRISM software (GraphPad Prism5) by using the one-way ANOVA with Tukey's multiple comparison *post hoc* test or the Chi-square test for multiple group analysis and the two-way ANOVA with Bonferroni post-tests for two variable analysis.

3. Results

3.1. SG formation upon acute oxidative stress in mutant ALS fibroblasts

To test whether mutations in different ALS causative genes may trigger different mechanisms of cell response to stress, we evaluated the formation of SG in fibroblasts from 3 healthy controls and ALS patients carrying mutations in *TARDBP* (p.A382T; mTDP-43, n = 3) and *C9ORF72* (mC9ORF72, n = 3) genes upon exposure to acute sub-lethal doses of ARS (0.5 mM for 30 min), as previously described in literature (Orrù et al., 2016). Immunostaining performed using TIAR as a SG marker revealed the formation of TIAR-positive cytoplasmic foci both in healthy control and mTDP-43 and mC9ORF72 fibroblasts, as expected (Fig. 1A). In contrast to what previously observed in immortalized cell lines (Colombrita et al., 2009), no colocalization of TDP-43 with TIAR in SG was observed in all cell groups, suggesting that TDP-43 is not recruited into these ribonucleoprotein complexes in primary fibroblasts following acute stress exposure (Fig. 1A).

To investigate potential differences between control and mutant ALS fibroblasts in stress response, a quantitative image analysis was performed. While only 24% control cells responded to acute ARS treatment by forming SG, mTDP-43 and mC9ORF72 fibroblasts showed a higher capability to form SG, with mC9ORF72 presenting significantly more cells forming SG (95%) with respect to mTDP-43 (56%) (Fig. 1B). Inter- and intra-patient variability in SG formation is shown in Supplementary Fig. S1. In order to evaluate toxicity induced by ARS treatment, we measured cell viability and found no evidence of cell death in both ARS-treated control and mC9ORF72 fibroblasts compared with the untreated samples (Fig. 1C). In contrast, a significant decreased cell viability (76%) was detected in mTDP-43 fibroblasts following acute ARS treatment in comparison with untreated cells (87%) (Fig. 1C).

As healthy control and mTDP-43 and mC9ORF72 ALS fibroblasts showed a different stress response to ARS treatment in terms of number

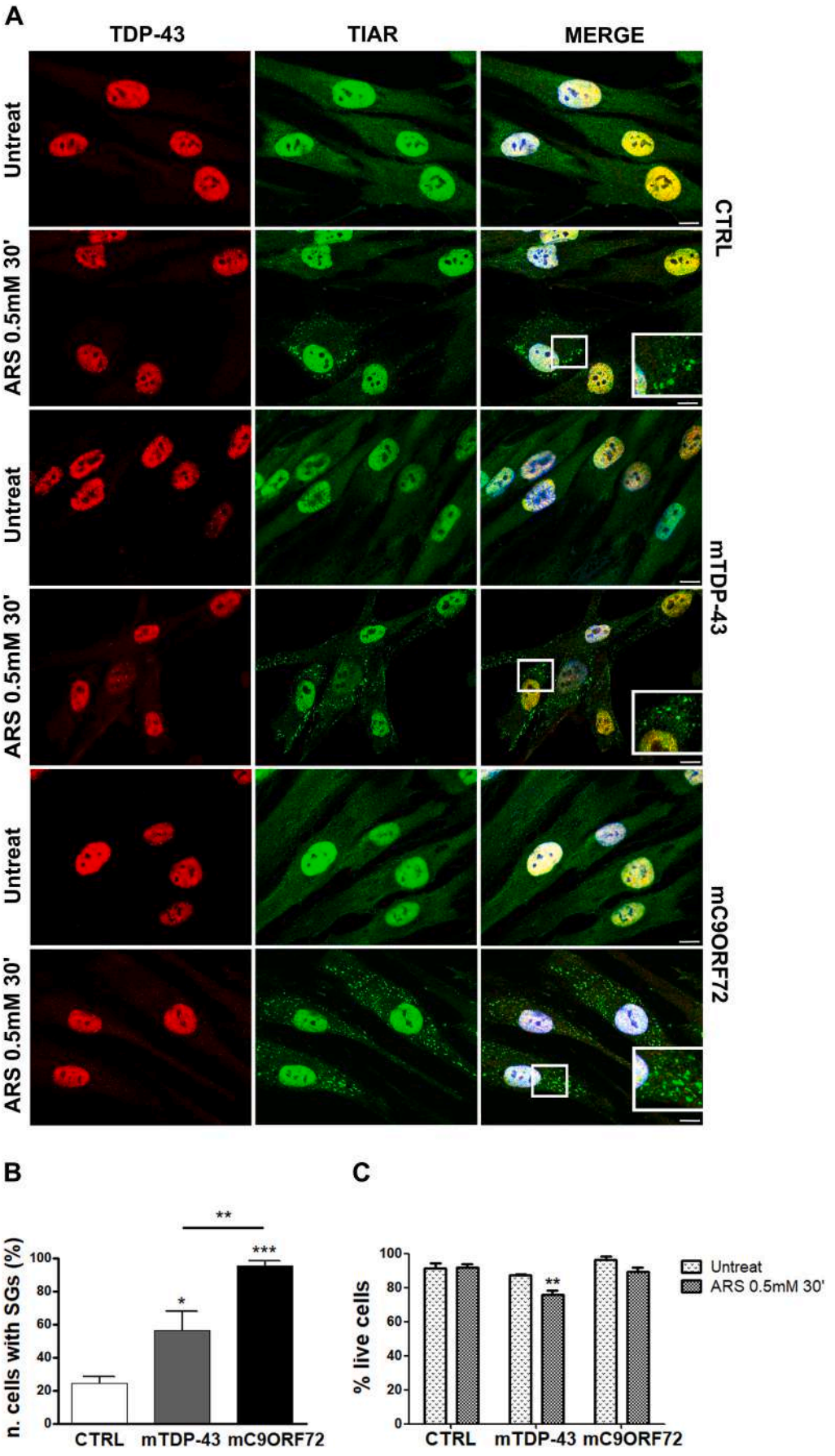

Fig. 1. TIAR-positive SG formation upon sub-lethal stress condition in healthy control and mutant ALS fibroblasts. A. Representative confocal images of TDP-43 (red) and the SG marker TIAR (green) in primary fibroblasts from 3 healthy controls (CTRL), 3 ALS patients carrying the *TARDBP* p.A382T mutation (mTDP-43) and 3 ALS patients with pathological hexanucleotide repeat expansion in *C9ORF72* gene (mC9ORF72), before (Untreat) and after acute sodium arsenite (ARS) treatment (0.5 mM for 30 min). Nuclei are stained in blue (DAPI) in all merged images. Box indicates enlarged area in inset. Bar, 10 μm. B. Quantitative analysis by ImageJ software of number of cells forming SG ($\geq 0.75\mu m^2$) upon acute ARS conditions in CTRL, mTDP-43 and mC9ORF72 fibroblasts (mean ± SEM, $n = 3$ individuals per each group of fibroblasts, experiments were repeated 2–4 times for each subject and at least 60 cells per sample were analyzed; one-way ANOVA with Tukey's multiple comparison *post hoc* test; $^{*}p < 0.05$ and $^{***}p < 0.001$ *vs* CTRL, $^{**}p < 0.01$ mC9ORF72 *vs* mTDP-43). C. Cell viability assessed by Trypan blue stain by using LunaII instrument (mean ± SEM, n = 3 individuals per each fibroblast group, experiments were repeated 2–3 times for each subject; two-way ANOVA with Bonferroni post-tests; $^{**}p < 0.01$ *vs* untreated sample). (For interpretation of the references to colour in this figure legend, the reader is referred to the web version of this article.)

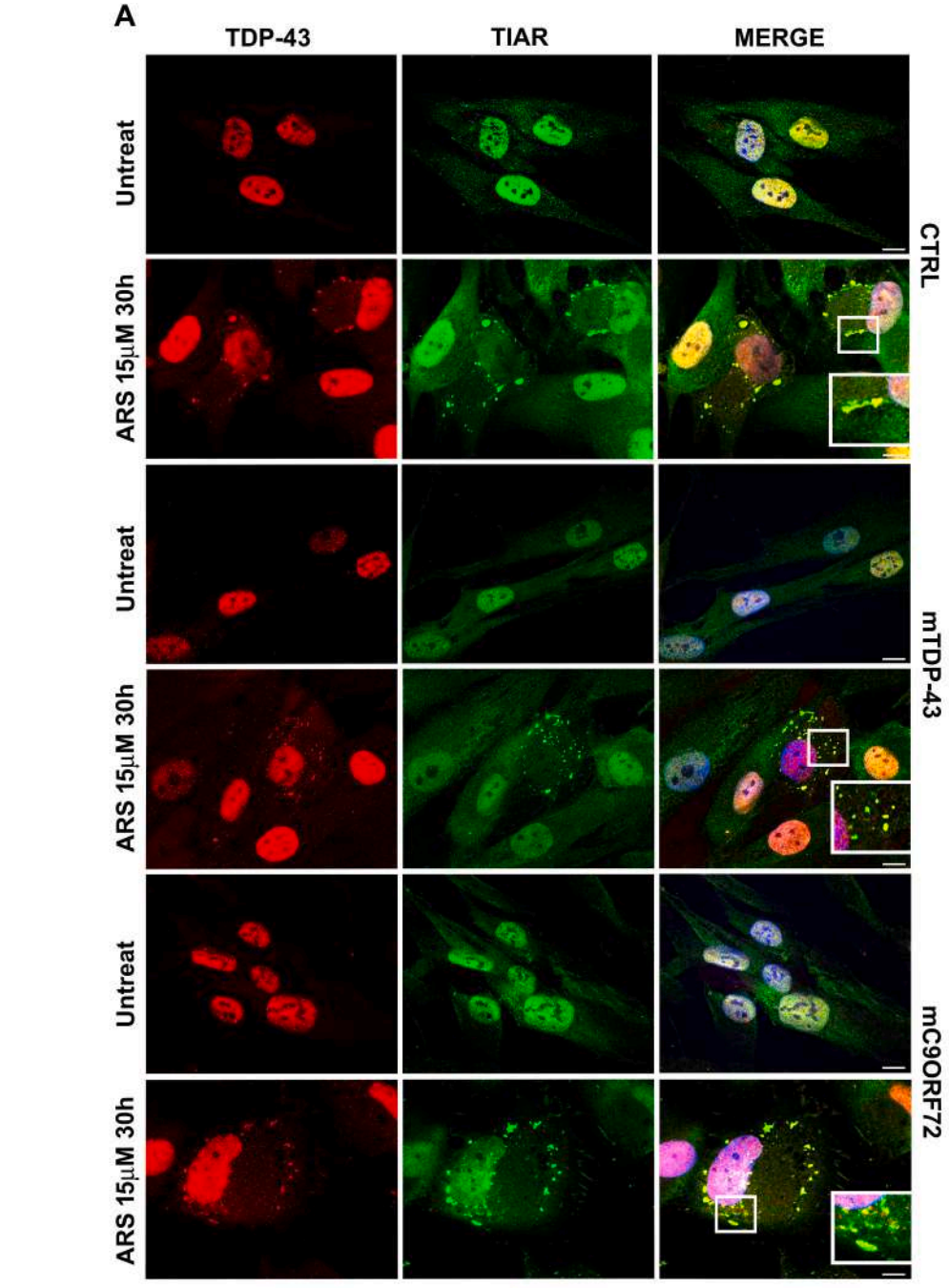

(caption on next page)

Fig. 2. TIAR-positive SG formation upon chronic stress condition in healthy control and mutant ALS fibroblasts. A. Representative confocal images of TDP-43 (red) and TIAR (green) in primary fibroblasts from CTRL, mTDP-43 and mC9ORF72 ALS patients, before (Untreat) and after chronic ARS treatment (15 μM for 30 h). Nuclei are stained in blue (DAPI) in all merged images. Box indicates enlarged area in inset. Bar, 10 μm. B. Time-course of stress response to 15 μM ARS for 6–48 h in healthy control fibroblasts (mean ± SEM, n = 3 individuals; one-way ANOVA with Tukey's multiple comparison *post hoc* test; *p < 0.05 30 h- *vs* 20 h-treatment and ***p < 0.001 *vs* all other timepoints). C. Quantitative analysis by ImageJ software of number of cells forming SG (≥0.75μm^2) upon chronic ARS conditions in CTRL, mTDP-43 and mC9ORF72 fibroblasts (mean ± SEM, n = 3 individuals per each fibroblast group, experiments were repeated 2–5 times for each subject and at least 60 cells per sample were analyzed; one-way ANOVA with Tukey's multiple comparison *post hoc* test; *p < 0.05 *vs* CTRL). D. Cell viability assessed by Trypan blue stain by using LunaII instrument (mean ± SEM, n = 3 individuals per each group of fibroblasts, experiments were repeated 2–3 times for each subject; two-way ANOVA with Bonferroni post-tests; *p < 0.05 *vs* untreated sample). (For interpretation of the references to colour in this figure legend, the reader is referred to the web version of this article.)

of cells forming SG, we investigated if they had also a different capability to dissolve SG upon stress removal. When we restored normal cell growth conditions for 2 h after acute ARS treatment, we observed the complete disappearance of any cytoplasmic granules, with no differences in stress recovery between healthy control and both mutant ALS fibroblasts (Supplementary Fig. S2).

These results suggest that mutant ALS fibroblasts are more vulnerable to acute oxidative stress than healthy control cells and that, unlike in immortalized cell lines, TDP-43 is not recruited into SG in primary fibroblasts.

3.2. SG formation upon prolonged oxidative stress in mutant ALS fibroblasts

To investigate the hypothesis that pathological inclusions containing TDP-43 protein in ALS/FTD autoptic brain tissues do derive from SG, we reproduced a milder and prolonged status of stress *in vitro* and evaluated if SG are able to form also in a condition which is more likely to occur during the neurodegenerative process, and not only under short and sub-lethal environmental insults as described in literature so far.

We first studied SG formation in healthy control fibroblasts which were exposed to different doses of ARS (15 and 50 μM) and for different timeframes (see Materials and Methods). When we treated cells with 15 μM ARS, we observed the formation of TIAR-positive SG at 15-h treatment with the maximum response in terms of number of cells with SG at 30 h (Fig. 2A-B). The treatment with higher doses (50 μM ARS for 6 h) did not induce SG formation and was toxic to cells at 16 h (data not shown).

In order to investigate whether mutations in ALS causative genes may influence cell response to prolonged stress in a gene-specific manner, similarly to what observed upon acute stress, we also exposed mTDP-43 and mC9ORF72 fibroblasts to the chronic ARS treatment (15 μM for 30 h) at which we observed the maximum formation of SG in healthy control fibroblasts (Fig. 2A-B). Both mutant ALS fibroblasts formed SG in this condition (Fig. 2A). No significant differences in terms of number of cells forming SG were observed in mC9ORF72 (36%) compared to control fibroblasts (45%), while a significant lower number of SG-positive cells was observed in mTDP-43 fibroblasts (23%) (Fig. 2C). Full data showing inter- and intra-patient variability in SG formation are reported in Supplementary Fig. S1. Interestingly, in contrast to what occurring upon the acute oxidative stress, we observed the recruitment of TDP-43 in SG forming in response to prolonged ARS treatment, as revealed by its co-localization with TIAR marker in both control and mutant mTDP-43 and mC9ORF72 fibroblasts (Fig. 2A). In particular, a colocalization image analysis revealed a strong positive correlation for TDP-43 and TIAR proteins (Pearson's coefficient values $r > 0.7$) in all sample cells with no significant differences (Supplementary Fig. S3).

Similarly to acute ARS treatment, also the prolonged 15 μM ARS exposure for 30 h did not decrease cell viability neither in healthy control nor in mC9ORF72 fibroblasts compared with the untreated samples, while treated mTDP-43 cells showed a significant decreased viability (77%) in comparison with untreated mTDP-43 fibroblasts (87%) (Fig. 2D). In all fibroblasts groups a bigger cell size was observed after chronic insult in comparison with the acute ARS treatment (Figs. 1A and 2A), suggesting a potential different metabolic activity upon prolonged stress exposure.

We investigated whether SG formation in condition of prolonged stress is a still reversible process. After 30-h ARS exposure, we restored normal cell growth condition for a time-course ranging from 24 to 72 h (Fig. 3A). A gradual decreased number of SG-forming cells was observed at 24 and 48 h in both healthy control and mC9ORF72 fibroblasts with the complete disassembly of SG at 72 h, while complete recovery of SG was already documented at 24 h in mTDP-43 cells (Fig. 3A-B).

To further prolong the exposure to oxidative stress, a lower concentration of ARS (5 μM) was tested for a time frame ranging from 24 h to 8 days (see Materials and Methods). While this condition did not show any effect on SG formation until 96 h (data not shown), treatment for 8 days induced TDP-43 mislocalization in the cytoplasm with TDP-43-positive, but TIAR-negative, cytoplasmic foci, being TIAR marker largely diffused in the nucleus and cytoplasm in both control and mutant ALS fibroblasts (Supplementary Fig. S4).

These results altogether suggest that not only the acute, but also a chronic oxidative insult is able to induce SG formation in primary fibroblasts, although at a different extent as mTDP-43 cells form less SG in comparison with controls. We found that the recruitment of TDP-43 protein into SG always occurs upon chronic stress regardless of the ALS disease condition and the gene mutation carried.

3.3. Differential formation of cytoplasmic granules upon acute and chronic oxidative stress

We observed that both mTDP-43 and mC9ORF72 fibroblasts showed significantly less cells forming SG in response to chronic *versus* acute ARS exposure (Fig. 4A). When we quantified the amount of cytoplasmic TIAR-positive granules, no differences were observed between control and mTDP-43 cells upon both oxidative stress insults (Fig. 4B). Conversely, we measured a significant increased number of granules per cell in mC9ORF72 fibroblasts (32 granules/cell) compared to the control group (20 granules/cell) only upon acute ARS exposure because this increase was not recapitulated after prolonged ARS treatment (18 *vs* 19 granules/cell in mC9ORF72 and controls, respectively) (Fig. 4B).

Our immunofluorescence analyses seemed to reveal a bigger SG size after the chronic oxidative stress than after the acute stress exposure (Fig. 1A and 2A). We therefore performed a quantitative image analysis of cytoplasmic granules size considering three arbitrary categories (0.1- < 0.75, 0.75–5 and > 5 μm^2), according to previous literature data, where SG were identified as having a size ≥0.75 μm^2 (Anderson, 2009; Aulas et al., 2015; Orrù et al., 2016). No differences in granule size distribution were detected among control, mTDP-43 and mC9ORF72 fibroblasts within the same stress condition (Fig. 4C). However, upon chronic stress we observed a significant increase in the number of SG belonging to both the two size categories 0.75-5 μm^2 (24% in acute *versus* 41% in chronic stress) and > 5 μm^2 (1% in acute *versus* 9% in prolonged stress), indicating an overall increase of SG size in this condition (Fig. 4D).

Our quantitative analysis reveals differences in terms of number of cells forming SG and of granules size between acute and chronic stress conditions in primary fibroblasts. This result, together with the

observation that TDP-43 is recruited in SG only upon a chronic insult, suggests also a different composition of cytoplasmic foci forming in the two stress conditions.

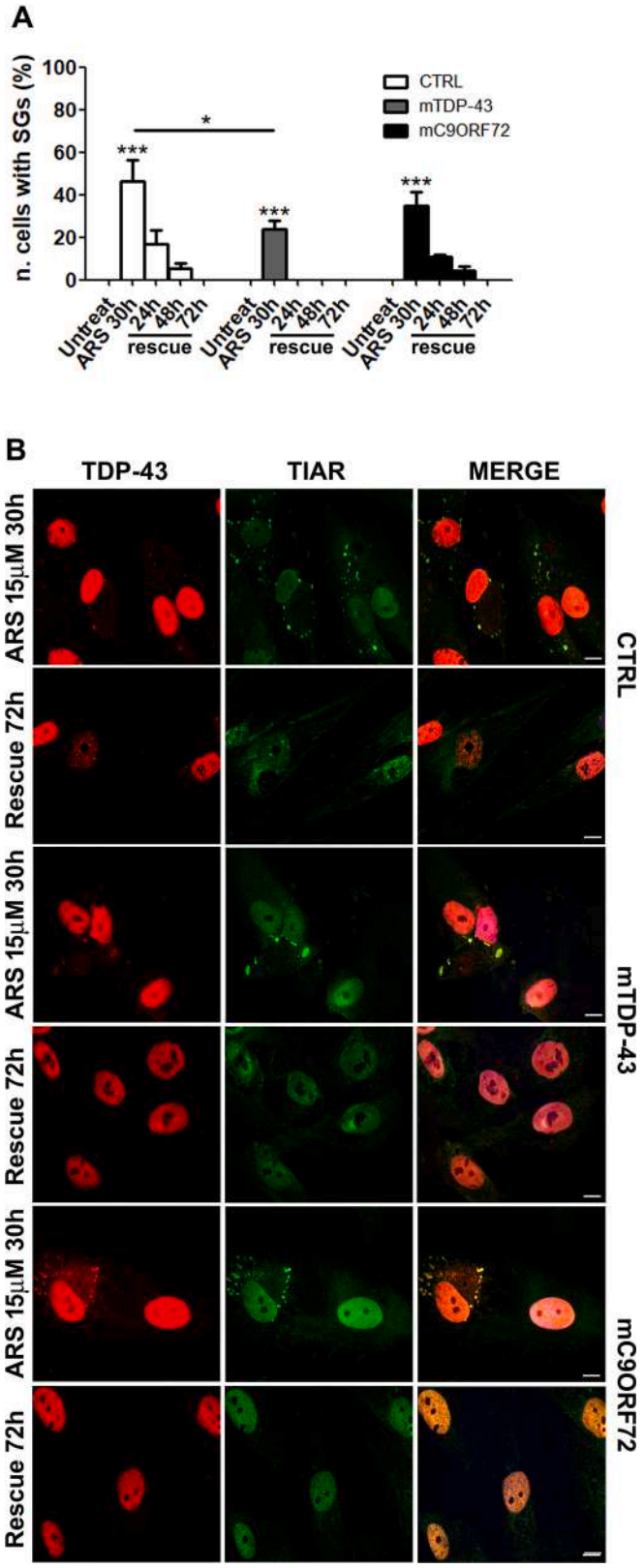

Fig. 3. Recovery experiments from chronic ARS treatment. A. Rescue experiments in CTRL and mTDP-43 and mC9ORF72 ALS fibroblasts treated with ARS 15 μM for 30 h and then grown in normal cell medium for a time-course ranging from 24 to 72 h (mean ± SEM, n = 3 individuals per each fibroblast group; two way ANOVA with Bonferroni post-tests; ***p < 0.001 *vs* untreated sample and all recovery conditions; *p < 0.05 mTDP-43 *vs* CTRL at 30 h-treatment). B. Representative confocal images of TDP-43 (red) and TIAR (green) in primary fibroblasts from 3 healthy CTRL, 3 mTDP-43 and 3 mC9ORF72 ALS patients in condition of chronic ARS treatment (15 μM for 30 h) and in condition of recovery for 72 h. Nuclei are stained in blue (DAPI) in all merged images. Bar, 10 μm. (For interpretation of the references to colour in this figure legend, the reader is referred to the web version of this article.)

3.4. Presence of phosphorylated TDP-43 aggregates in cells exposed to chronic oxidative stress

We investigated whether TDP-43 protein recruited into SG under prolonged oxidative stress was phosphorylated at Ser 409/410, since abnormal phosphorylation of TDP-43 was reported in ALS/FTD pathological aggregates (Neumann et al., 2009, 2006). We found that mTDP-43 and mC9ORF72 fibroblasts showed P-TDP-43-positive filaments or a P-TDP-43 granular distribution in the cytoplasm in both physiological and acute stress conditions, while P-TDP-43 protein expression was very low in control cells (Fig. 5A). Moreover, after acute ARS exposure, no localization of P-TDP-43 was observed in TIAR-positive SG in both control and all mutant ALS fibroblasts (Fig. 5A). However, under prolonged ARS treatment, we observed the formation of cytoplasmic P-TDP-43 aggregates, distinct from SG, with a filamentous or, more frequently, a round shape, similar to the TDP-43 pathological inclusions found in ALS/FTD autoptic brain tissues (Fig. 5A). In particular, healthy control (23%) and mTDP-43 (15%) fibroblasts showed a similar formation of P-TDP-43-positive aggregates, while a significant higher number of mC9ORF72 cells (70%) presented cytoplasmic P-TDP-43 aggregates (Fig. 5B). In untreated conditions, such P-TDP-43 aggregates were present only in few cells from both control (2%) and mutant ALS patients (4% mTDP-43 and 5% mC9ORF72) (Fig. 5B).

When we quantified the number of cells presenting both SG and P-TDP-43 aggregates in condition of chronic oxidative stress, we found that not all cells presenting P-TDP-43 aggregates contained also SG (18% double-positive *vs* 23% P-TDP-43-positive cells in controls, 10% *vs* 15% in mTDP-43, 24% *vs* 70% in mC9ORF72) and that mTDP-43 fibroblasts showed a significant smaller content of double-positive cells compared to mC9ORF72 cells (Fig. 5C-D). By comparing data on SG formation (Fig. 2C), we observed that control and mTDP-43 fibroblasts formed more SG than P-TDP-43 aggregates (45% SG *vs* 23% P-TDP-43 aggregates in controls; 23% SG *vs* 15% P-TDP-43 aggregates in mTDP-43), while we observed an opposite response in mC9ORF72 cells (36% SG *vs* 70% P-TD-43 with 24% of double-positive cells), suggesting that SG and P-TDP-43 aggregates may form within the same cell but also independently upon chronic stress (Fig. 5D).

However, when chronic stress was removed, a complete disassembly of P-TDP-43 cytoplasmic aggregates was observed after 72-h recovery together with SG, with P-TDP-43 being very low expressed in the nucleus in all fibroblast groups and no longer forming cytoplasmic filaments as in the original untreated ALS fibroblasts (Fig. 3 and 5A).

These findings show that, in ALS patient-derived fibroblasts upon condition of chronic stress, the recruitment of TDP-43 protein into SG and the formation of cytoplasmic P-TDP-43 aggregates may occur concurrently or as an independent event, suggesting a potential interplay between these two structures. As P-TDP-43 aggregates are much more abundant than SG in mC9ORF72 cells, while the contrary is observed in healthy control and mTDP-43 patients, our results suggest that the ALS-associated genetic background may exert a strong influence on cell stress response.

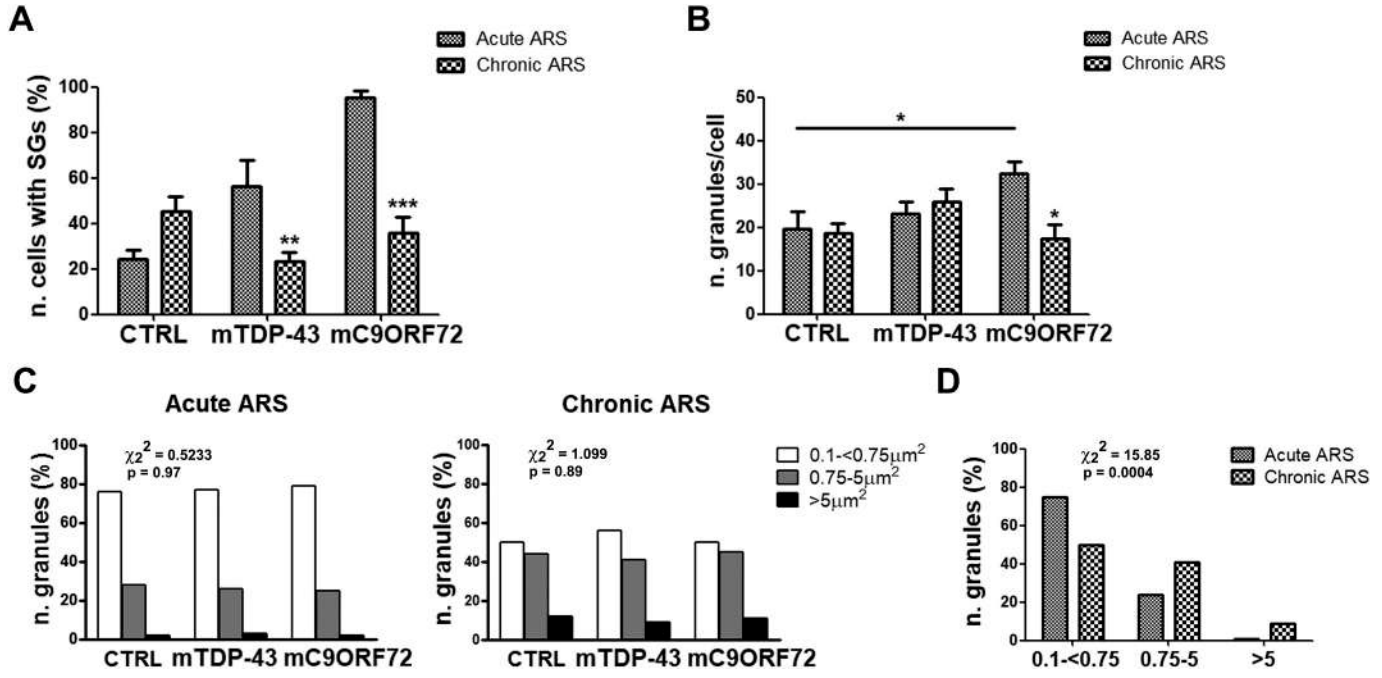

Fig. 4. Differences in granules size and number upon acute and prolonged stress exposure. A. Quantitative analysis by ImageJ software of number of cells forming SG ($\geq 0.75\mu m^2$) upon chronic ARS conditions (15 μM 30 h) in comparison to acute ARS treatment (0.5 mM 30′) in CTRL, mTDP-43 and mC9ORF72 fibroblasts (mean ± SEM, n = 3 individuals per each group of fibroblasts, experiments were repeated 2–5 times for each subject and at least 60 cells per sample were analyzed; two-way ANOVA with Bonferroni post-tests; **p < 0.01 and ***p < 0.001 *vs* acute ARS treatment). B. Quantitative image analyses by ImageJ software of granules number/cell in CTRL, mTDP-43 and mC9ORF72 fibroblasts upon acute and chronic stress conditions (two-way ANOVA with Bonferroni post-tests; *p < 0.05). C. Quantitative image analyses by ImageJ software of granules size in CTRL, mTDP-43 and mC9ORF72 fibroblasts after acute *(left panel)* and chronic stress *(right panel)* exposure. Three interval values were arbitrarily considered (0.1- < 0.75 μm^2, 0.75-5 μm^2, > 5 μm^2) and granules distribution in the three different classes was evaluated for each fibroblast group (mean, n = 3 individuals per each fibroblast group; experiments were repeated 2–5 times for each subject and at least 60 cells per sample were analyzed; Chi-square test; $\chi_2^2 = 0.5233$, $p = 0.97$ for acute treatment; $\chi_2^2 = 1.099$, $p = 0.89$ for chronic treatment). D. Graph showing the comparison in terms of granules size distribution between acute and chronic ARS treatment. CTRL, mTDP-43 and mC9ORF72 fibroblasts were collapsed in one group as no differences emerged between the 3 groups in terms of granules size within the same stress condition (mean, Chi square test; $\chi_2^2 = 15.85$, $p = 0.0004$).

3.5. Impairment of the autophagy pathway upon chronic stress

The formation of TDP-43 pathological inclusions during the neurodegenerative process in ALS/FTD has been hypothesized to derive from a failure of SG to properly disassemble in condition of a prolonged insult, as a consequence of an impairment of the autophagy pathway (Monahan et al., 2016). We therefore analyzed the levels of p62, an autophagy cargo receptor used as a marker of autophagy progression. By immunofluorescence analysis, we observed low levels of p62 in both control and mTDP-43 and mC9ORF72 ALS fibroblasts under physiological conditions and acute ARS treatment (Fig. 6A). A great increase and accumulation of p62 was instead observed upon chronic oxidative stress, with no significant differences among all fibroblast groups (84% of healthy control cells, 74% of mTDP-43 and 90% of mC9ORF72 cells) (Fig. 6A-B). The analysis of the number of cells containing both SG and p62 aggregates revealed that, under chronic stress condition, most cells forming SG were positive for p62 aggregates in both healthy control (42% double-positive cells *vs* 45% TIAR-positive SG) and mutant ALS fibroblast groups (17% double-positive cells *vs* 23% TIAR-positive SG in mTDP-43 and 29% double-positive cells *vs* 36% TIAR-positive SG in mC9ORF72 cells) (Fig. 6C). Interestingly, in SG-containing cells, p62 appeared distinct from TIAR-positive SG, although in some cases we observed co-localization (Fig. 6A). Following chronic stress removal, we still observed small aggregates of p62 in roughly 15% of all cells at 72-h recovery, when P-TDP-43 aggregates and SG had completely disappeared (Fig. 6A).

Since C9ORF72 protein is involved in autophagy (Wang et al., 2020) and mC9ORF72 fibroblasts show a high formation of cytoplasmic P-TDP-43 aggregates (Fig. 5B-D) compared to control and mTDP-43 cells, we further investigated the connection of the autophagy pathway with cell response to prolonged stress in mC9ORF72 fibroblasts by performing an ultrastructural analysis, which is considered a gold standard approach to evaluate autophagy. We observed cytoplasmic multishaped structures, containing fibrillar patches stained with TIAR without limiting membranes and sometime also positive for p62 immune-gold particles, in control and mC9ORF72 fibroblasts treated with chronic ARS (Fig. 6D), and absent in untreated cells. The involvement of autophagy pathway in SG dynamics after chronic oxidative stress was evaluated by counting the number of both p62-TIAR and LC3-TIAR immune-positive autophagic vacuoles, being LC3 a marker of autophagy vesicle formation and maturation. A similar increase in the number of p62-TIAR double-stained vacuoles was observed in both ARS-treated control (2,3 vacuoles/cell) and mC9ORF72 (2 vacuoles/cell) fibroblasts compared to untreated cells (0,4 and 0,5 vacuoles/cell in control and mC9ORF72 fibroblasts, respectively) (Fig. 6E-F). Likewise, we detected a significantly increased number of LC3-TIAR-positive vacuoles after chronic ARS exposure in both control (1,6 *vs* 0,5 in untreated controls) and mC9ORF72 fibroblasts (0,9 *vs* 0,5 in untreated mC9ORF72) (Supplementary Fig. S5). However, the number of double-labeled LC3-TIAR vacuoles was significantly lower in mC9ORF72 fibroblasts compared to healthy control ones, supporting the evidence that C9ORF72 haploinsufficiency occurring in mutant *C9ORF72* ALS patients impairs autophagy (Chitiprolu et al., 2018; Webster et al., 2016).

These results show that formation of SG and P-TDP-43 aggregates in condition of chronic oxidative stress is concomitant with a significant increase and accumulation of p62 in a very high percentage of cells in all fibroblast groups. However, while SG and P-TDP-43-positive aggregates completely dissolved in fibroblasts after 72-h recovery from chronic stress, smaller p62 aggregates still persisted, supporting that

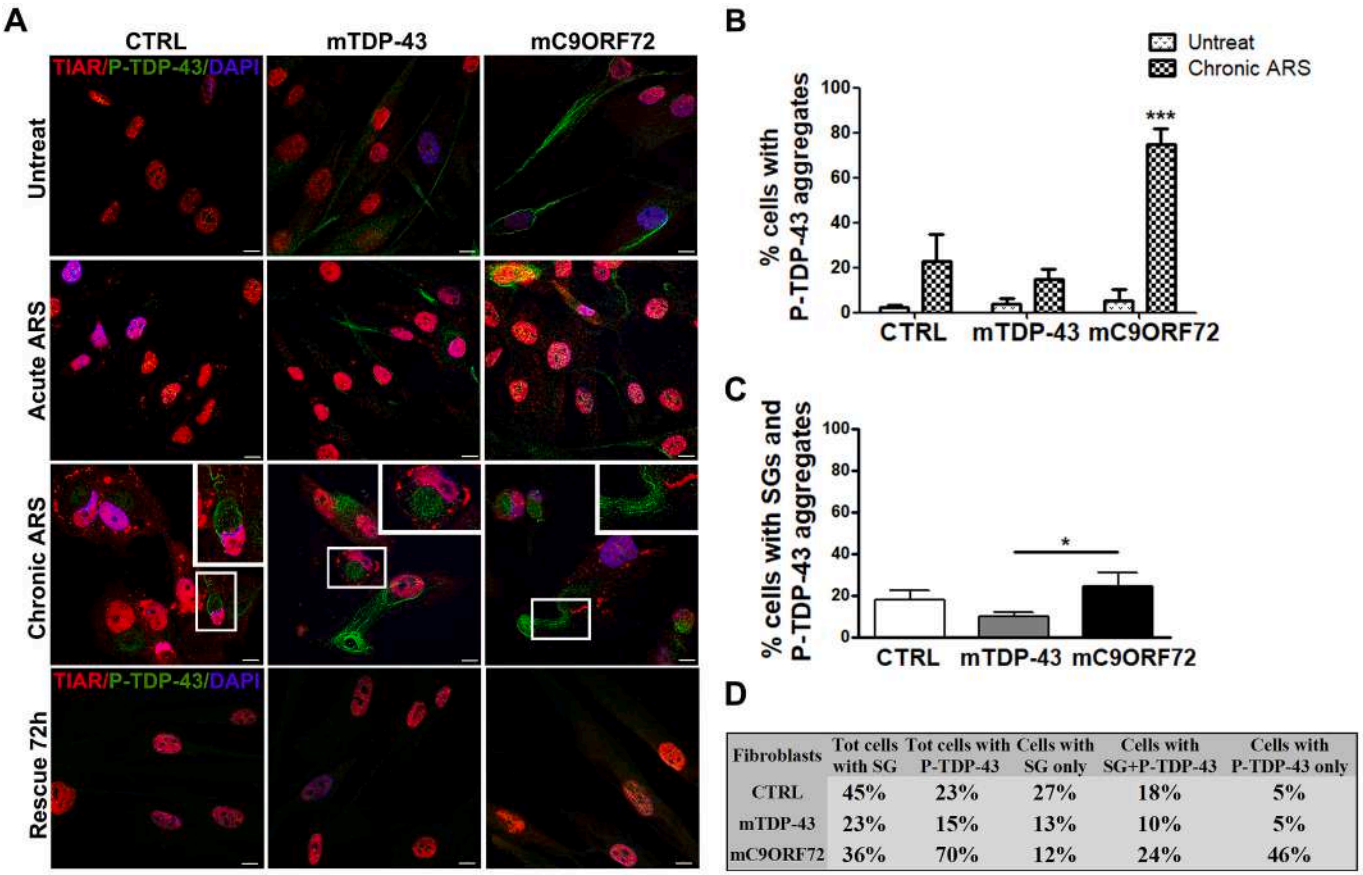

Fibroblasts	Tot cells with SG	Tot cells with P-TDP-43	Cells with SG only	Cells with SG+P-TDP-43	Cells with P-TDP-43 only
CTRL	45%	23%	27%	18%	5%
mTDP-43	23%	15%	13%	10%	5%
mC9ORF72	36%	70%	12%	24%	46%

Fig. 5. Analysis of TDP-43 phosphorylation in ALS patients' fibroblasts during cellular response to prolonged stress. A. Representative confocal images of TIAR (red) and TDP-43 phosphorylated at Ser409/410 (P-TDP-43, green) in primary fibroblasts from CTRL and ALS patients (mTDP-43 and mC9ORF72), in untreated, acute (0.5 mM 30 min), chronic (15 μM 30 h) ARS-treated cells and after 72-h recovery from chronic ARS exposure. Nuclei are stained in blue (DAPI) in all merged images. Box indicates enlarged area in inset. Bar, 10 μm. B. Quantitative analysis of the number of fibroblasts (%) with P-TDP-43 aggregates in CTRL, mTDP-43 and mC9ORF72 patients in untreated and chronic ARS conditions (mean ± SEM, n = 3 individuals per each group of fibroblasts; at least 60 cells per sample were analyzed; two-way ANOVA with Bonferroni post-tests; ***p < 0.001 *vs* Untreat and *vs* other groups). C. Quantitative analysis of the number of SG- and P-TDP-43 aggregates-positive cells (%) in CTRL, mTDP-43 and mC9ORF72 ALS patients in chronic ARS conditions (mean ± SEM, n = 3 individuals per each group of fibroblasts; at least 60 cells per sample were analyzed; one-way ANOVA with Tukey's multiple comparison *post hoc* test; *p < 0.05 *vs* mC9ORF72). D. Table summarizing data about SG and P-TDP-43 aggregates formation in fibroblasts under condition of chronic oxidative stress. (For interpretation of the references to colour in this figure legend, the reader is referred to the web version of this article.)

prolonged oxidative stress impairs autophagy and a defective autophagy system may gradually contribute to an impairment of the protein quality control. The increased number of p62-TIAR- and LC3-TIAR-positive autophagic vacuoles reinforces also the idea that p62, through autophagy, plays a direct and pivotal role in efficient SG clearance.

3.6. Analysis of cellular response to acute and chronic oxidative stress in ALS iPSC-derived motoneurons

To investigate if features of cell stress response were maintained also in neuronal cells, which are mainly affected in the pathology, we analyzed SG formation in iPSC-derived motoneurons (iPSC-MN) obtained after reprogramming and differentiation of the same healthy control and ALS patients' fibroblasts (Fig. 7A, Supplementary Table S1 and Supplementary Fig. S6).

After acute ARS treatment we observed the formation of TIAR-positive SG, as already reported in literature (Lenzi et al., 2015), which were present in 100% of both control and mutant mTDP-43 and mC9ORF72 ALS iPSC-MN (Supplementary Fig. S6 and Fig. 7B), contrarily to fibroblasts (Fig. 1). In all iPSC-MN, regardless their genotype, TDP-43 did not co-localize with SG upon acute oxidative stress (Fig. 7B), similarly to what previously described in fibroblasts (Fig.1).

To set up the chronic stress condition in iPSC-MN, we first exposed cells to the same treatment used for fibroblasts (15 μM ARS). However, this treatment was toxic to iPSC-MN already at 24 h, while it was not able to induce SG formation in a shorter time interval (16 h) (data not shown). Therefore, iPSC-MN were subsequently exposed to lower doses of ARS (see Materials and Methods) and we found that a treatment with 10 μM ARS for 24 h was able to induce SG formation, although to a smaller extent than in fibroblasts, without differences between healthy control (13%) and mutant ALS iPSC-MN (12% mTDP-43 and 16% mC9ORF72) (Fig. 7C-D). Interestingly, also iPSC-MN showed the recruitment of TDP-43 into SG after a prolonged stress (Fig. 7C), similarly to what we observed in primary fibroblasts (Fig. 2).

We further investigated the response of iPSC-MN to chronic oxidative stress by analyzing P-TDP-43 and p62 markers. In physiological conditions, P-TDP-43 protein was very low expressed (Fig. 7E) and small deposits of P-TDP-43 were observed only in few iPSC-MN from both control (10%) and mutant ALS patients (12% and 9% of untreated mTDP-43 and mC9ORF72 cells, respectively) (Supplementary Fig. S7). Under chronic ARS condition, instead, immunostaining assay showed the presence of the phosphorylated protein in big cytoplasmic aggregates with a round shape (Fig. 7E-G), similar to the P-TDP-43 inclusions previously observed in fibroblasts (Fig. 5A), both in control (44%) and in mTDP-43 (50%) and mC9ORF72 (45%) iPSC-MN with no significant differences (Fig. 7E-G). Compared to primary fibroblasts

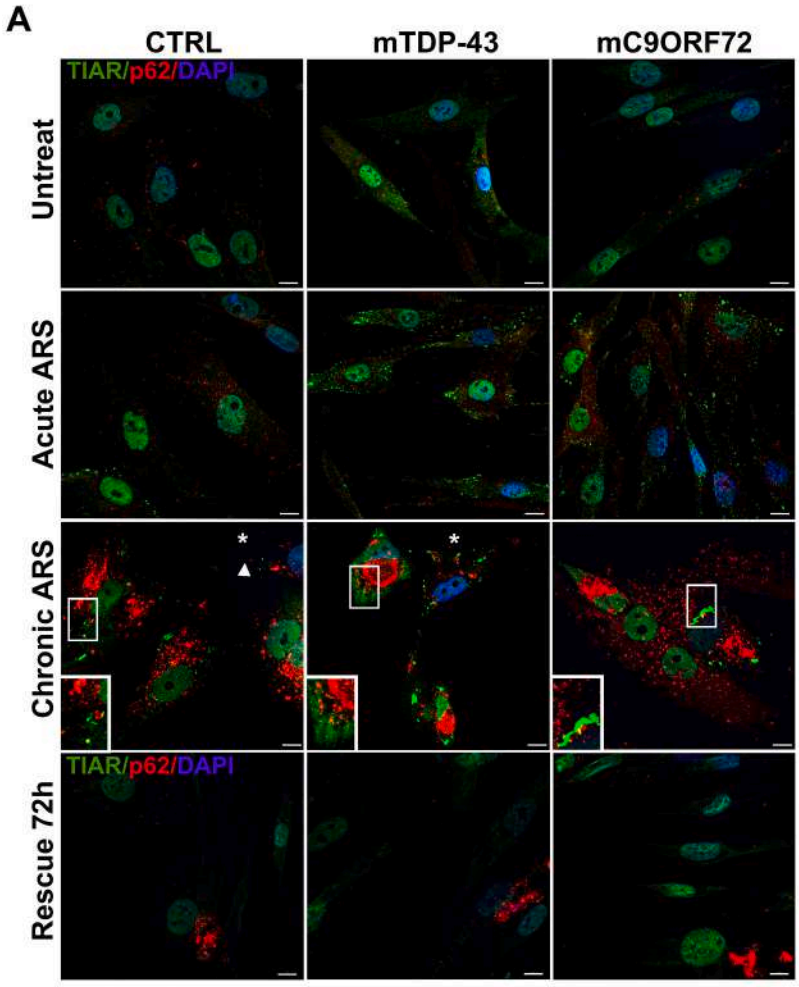

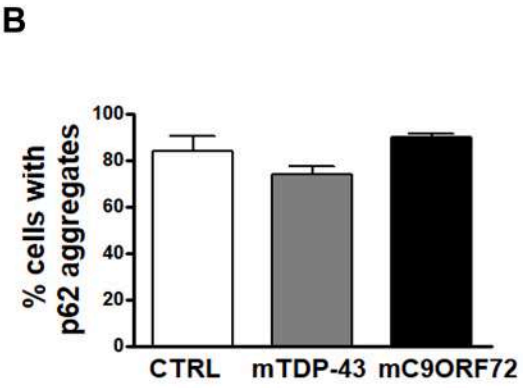

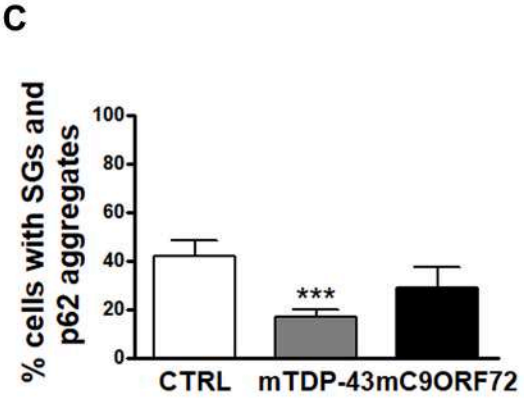

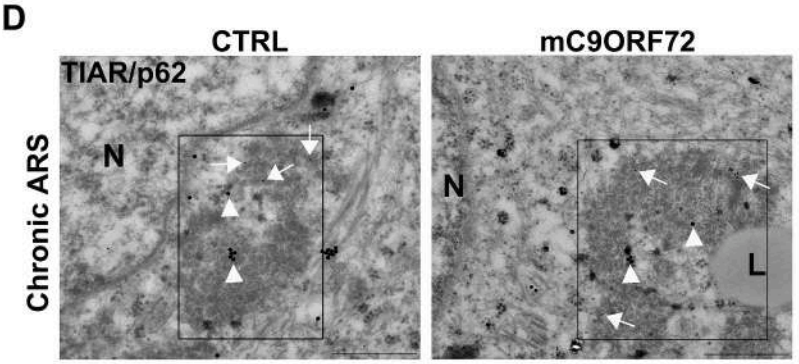

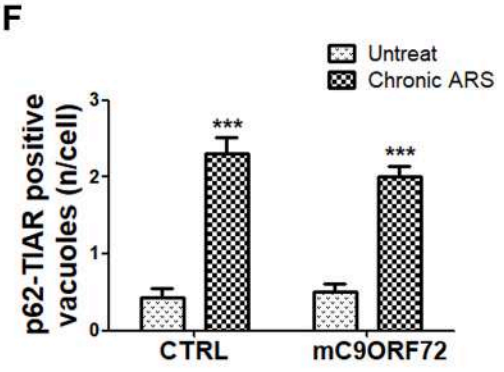

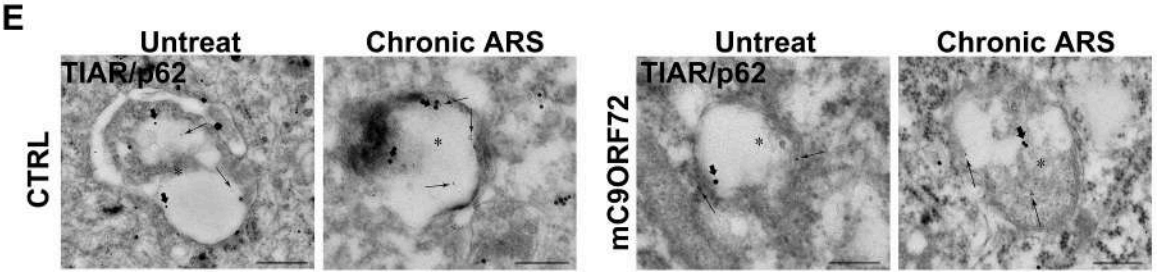

(caption on next page)

Fig. 6. Characterization of cellular stress response by investigation of the autophagic pathway. A. Representative confocal images of TIAR (green) and the autophagic receptor p62 (red) in primary fibroblasts from 3 CTRL, 3 mTDP-43 and 3 mC9ORF72 ALS patients, in untreated, acute (0.5 mM 30 min), chronic (15 μM 30 h) ARS-treated conditions and after 72-h recovery from chronic ARS exposure. Nuclei are stained in blue (DAPI) in all merged images. Box indicates enlarged area in inset. Bar, 10 μm. B. Quantitative analysis of the number of fibroblasts (%) with p62 aggregates in CTRL, mTDP-43 and mC9ORF72 patients in condition of chronic ARS treatment (mean ± SEM, n = 3 individuals per each group of fibroblasts; at least 60 cells per sample were analyzed; one-way ANOVA with Tukey's multiple comparison *post hoc* test). C. Quantitative analysis of the number of cells (%) with both SG and p62 aggregates in chronic ARS conditions in CTRL, mTDP-43 and mC9ORF72 ALS patients (mean ± SEM, n = 3 individuals per each group of fibroblasts; at least 60 cells per sample were analyzed; one-way ANOVA with Tukey's multiple comparison *post hoc* test; ***p < 0.001 *vs* CTRL). D. Representative electron microscopy micrographs of SG in control and mC9ORF72 fibroblasts after chronic stress. SG appear as cytoplasmic multi-shaped structures, not surrounded by membranes and containing fibrillar patches, stained with TIAR (10 nm Ø; *arrows*) and p62 immune-gold particles (20 nm Ø; *arrowheads*). N = nucleus; L = lipid. 8.000× magnification. Scale bar: 400 nm. E. Representative micrographs of cytosolic autophagic vacuoles *(asterisks)* immunopositive for both p62 (20 nm Ø; *thick arrows*) and TIAR (10 nm Ø; *thin arrows*) from fibroblasts in physiological conditions and after chronic stress. Scale bar: 200 nm. F. The graph reports the number *per cell* of autophagic vacuoles positive for both p62 and TIAR in control and in mC9ORF72 fibroblasts in basal condition and after chronic ARS (mean ± SEM, *n* = 30 cells for each experimental group; two-way ANOVA; ***p < 0.001 *vs* Untreat). (For interpretation of the references to colour in this figure legend, the reader is referred to the web version of this article.)

(Fig. 5B), the number of iPSC-MN forming P-TDP-43 aggregates was higher than the number of cells forming SG (Fig. 7D-G). Importantly, in all iPSC-MN, no co-localization of P-TDP-43 aggregates with TIAR-positive SG was observed (Fig. 7E), similarly to what already reported in primary fibroblast cells (Fig. 5A).

After prolonged stress, the analysis of the autophagy marker p62 revealed the presence of abundant aggregates which were instead absent in untreated cells (Fig. 7F). Similarly to fibroblasts, the induction of p62 upon prolonged oxidative insult was higher than the induction of SG formation and of P-TDP-43 aggregates, with 71% control, 80% mTDP-43 and 63% mC9ORF72 iPSC-MN showing p62 aggregates, with no significant differences among cell groups (Fig. 7H). This suggests that, similarly to primary fibroblasts, chronic stress condition may lead to a dysregulation of the autophagy pathway also in iPSC-MN.

Altogether these results show that, not only the acute, but also a chronic oxidative insult is able to induce formation of SG and P-TDP-43 aggregates in iPSC-MN although at different extent compared to fibroblasts, and that iPSC-MN do not show the gene-specific differences observed in mutant ALS and control fibroblasts in cell stress response.

4. Discussion

In this study we demonstrate that a status of chronic oxidative stress is able to promote the formation of SG in primary fibroblasts and iPSC-MN from both healthy controls and ALS patients carrying different gene mutations. SG have been hypothesized to be precursors of TDP-43 pathological aggregates forming during the neurodegenerative process in ALS/FTD diseases (Monahan et al., 2016), although this issue is still under debate. In fact, almost all studies were so far performed administering sub-lethal and short-lasting stress conditions, which markedly differ from the chronic stress conditions occurring during neurodegeneration. In addition, most studies were carried out by using immortalized cell lines showing bias when translated to patients' cells. Our data in patient-derived cells also show that the recruitment of TDP-43 into SG occurs specifically in a chronic stress condition together with the formation of distinct cytoplasmic phosphorylated TDP-43 aggregates, very similar to the pathological inclusions observed in ALS/FTD brains.

When we compared cellular response to chronic stress with sub-lethal stress condition usually used in literature, we found that this response was different in terms of SG formation and size. In acute ARS conditions almost the totality of fibroblasts from mC9ORF72 and more than 50% of cells from mTDP-43 patients formed SG, while control fibroblasts were less responsive, suggesting that mutant ALS fibroblasts are more vulnerable to stress due to an increased susceptibility. Literature data support these results as, in condition of acute oxidative stress, ALS-linked mutations were described to enhance TDP-43 and FUS cytoplasmic translocation and SG formation in both human cell lines and animal models (Bosco et al., 2010; Gopal et al., 2017; Johnson et al., 2009; Liu-Yesucevitz et al., 2010; Mann et al., 2019; Schmidt and Rohatgi, 2016). On the contrary, a previous study on mTDP-43 fibroblasts showed that the same TDP-43 p.A382T mutation caused a significant decreased number of cells forming SG compared to controls in condition of acute stress (Orrù et al., 2016). Our study included a larger sample size and, importantly, we also showed that inter- and intra-patient variability was particularly relevant in response to acute oxidative stress in mTDP-43 fibroblasts. We therefore can not exclude that both variability and different clinical features of ALS patients may account for the different results previously reported (Orrù et al., 2016).

In contrast to acute stress conditions, when we reproduced a milder and prolonged status of chronic stress *in vitro*, fibroblasts from mTDP-43 patients formed less SG in comparison with control fibroblasts. We speculate that, when the stress persists becoming chronic as in neurodegeneration, mTDP-43 cells, in contrast to mC9ORF72, show less ability to induce a long-term protective mechanism. In line with this hypothesis, also cell viability is specifically reduced in mTDP-43 fibroblasts upon both acute and chronic stress exposure, supporting a higher vulnerability of these mutant *TARDBP* cells.

Our data also show that, regardless of the ALS condition and gene mutation carried, TDP-43 protein is recruited into SG only in response to chronic, but not to acute, oxidative insult in all cells, both fibroblasts and iPSC-MN. This is in contrast to what we and other groups previously described in immortalized cell lines where localization of TDP-43 in SG occurred under sub-lethal stress conditions (Birsa et al., 2019; Colombrita et al., 2009). The fact that primary fibroblasts and differentiated motoneuronal cells show a different response to stress compared to immortalized cell lines is also supported by a recent paper showing that TDP-43 is recruited into SG after 24-h puromycin treatment in mutant *TARDBP* p.N352S and *FUS* p.R521G iPSC-MN (Fang et al., 2019). These observations again underline the importance of studying and validating pathomechanisms in patient-derived cells to avoid bias when translating to humans.

Our analysis revealed a significant increase of SG size in all fibroblast groups in chronic compared to acute treatment, suggesting that, after a prolonged stress, both a fusion of smaller granules as well as a different composition of SG may occur, as already hypothesized (Mahboubi and Stochaj, 2017). An altered composition of SG and an increase of cytoplasmic TDP-43 protein, as described for ALS-linked mutations, may promote interactions between the LCD of several RBPs, aberrant phase transition and protein aggregation, finally triggering the neurodegenerative process in ALS/FTD and other neurodegenerative diseases (Daigle et al., 2013; Gopal et al., 2017; Hyman et al., 2014; McGurk et al., 2018; Molliex et al., 2015; Schmidt and Rohatgi, 2016; Wheeler et al., 2016). In this scenario a crosstalk between SG components and TDP-43 cytoplasmic aggregates may occur because of the intrinsic biophysical properties of SG, as their assembly *via* the liquid-liquid phase separation (LLPS) process from cytoplasm is mediated by the LCD contained in most RBPs (Gilks et al., 2004; Harrison and Shorter, 2017; Hyman et al., 2014; Wippich et al., 2013).

In our experimental condition of prolonged oxidative stress, the formation of SG was associated also to the contemporary presence of phospho-TDP-43 aggregates. In healthy control and mTDP-43 patients,

fibroblasts formed more SG than P-TDP-43 aggregates, while in mC9ORF72 cells we observed the opposite response, being the P-TDP-43 aggregates much more abundant than SG. However, this complex interplay between SG and TDP-43 inclusions seems to be cell-specific because in iPSC-MN we observed a different situation with P-TDP-43 aggregates being more abundant than SG, independently on disease condition and the gene mutation carried. Our findings therefore suggest that, in ALS patient-derived cells, TDP-43 protein inclusions may arise

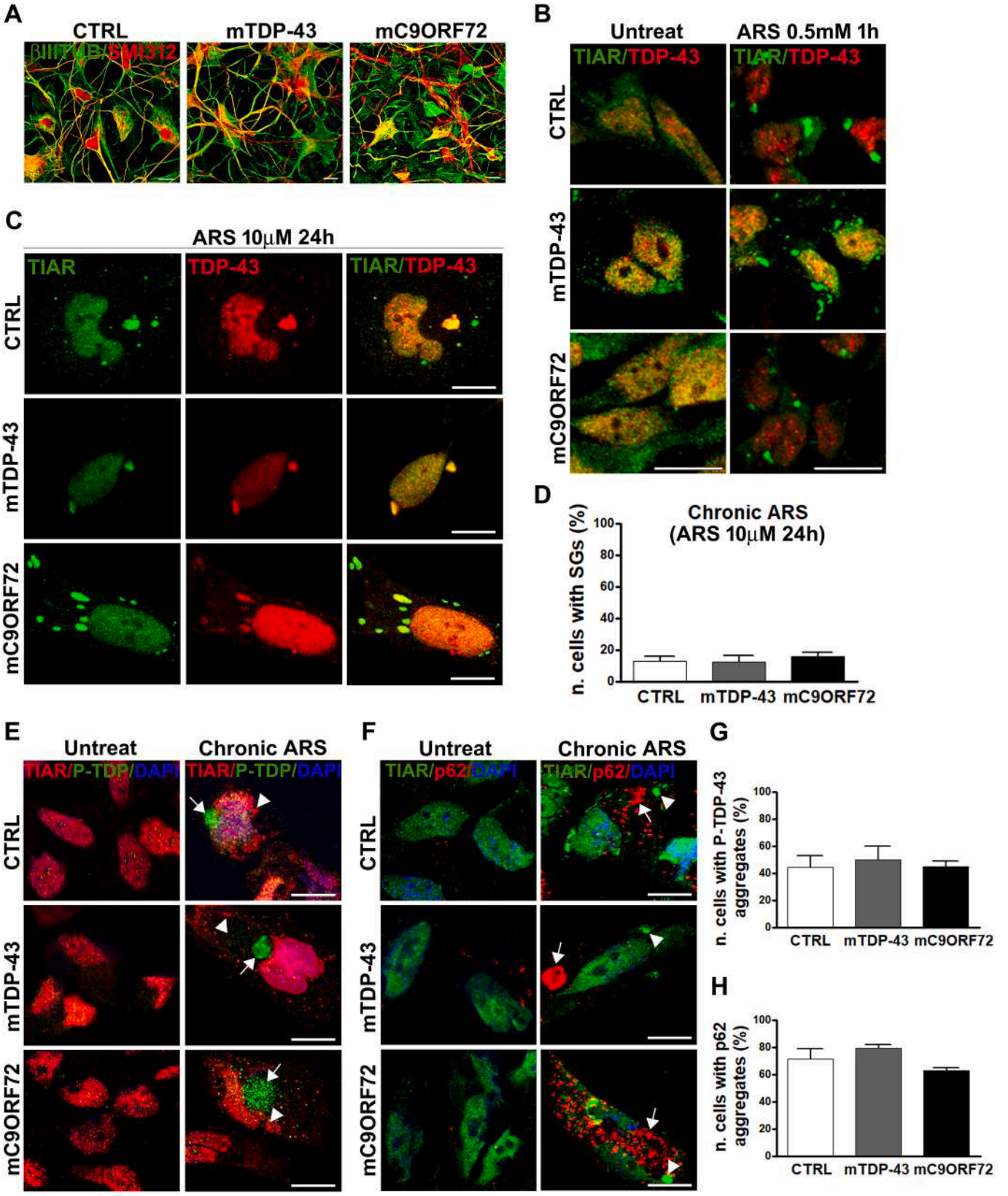

(caption on next page)

Fig. 7. SG formation and cellular response to acute and chronic stress conditions in iPSC-MN. A. Representative confocal images of βIII tubulin (green) and SMI312 (red) neuronal markers in differentiated iPSC-MN from 1 healthy CTRL and 1 mTDP-43 and 1 mC9ORF72 ALS patient. Bar, 10 μm. Representative confocal images of TIAR (green) and TDP-43 (red) in iPSC-MN from 1 CTRL and 1 mTDP-43 and 1 mC9ORF72 ALS patient (B) before and after acute stress conditions (0.5 mM ARS for 1 h) and (C) upon chronic ARS conditions (10 μM 24 h). Bar, 10 μm. D. Quantitative analysis by ImageJ software of numbers (%) of control and mutant ALS iPSC-MN forming SG upon chronic ARS conditions (mean ± SEM, $n = 2$ differentiations per each sample; at least 60 cells per sample were analyzed; one-way ANOVA with Tukey's multiple comparison *post hoc* test). Representative confocal images of (E) TIAR (red) and P-TDP-43 (Ser409/410; green) and of (F) TIAR (green) and p62 (red) in control and mutant iPSC-MN before and after chronic ARS treatment. Nuclei are stained in blue (DAPI) in all merged images. *Arrowhead* indicates SG, *arrow* indicates P-TDP-43 aggregates in (E) and p62 aggregates in (F), respectively. Bar, 10 μm. Quantitative analysis of the number (%) of iPSC-MN with P-TDP-43 aggregates (G) and p62 aggregates (H) after chronic ARS treatment (mean ± SEM, n = 2 differentiations per each sample; at least 60 cells per sample were analyzed; one-way ANOVA with Tukey's multiple comparison *post hoc* test). (For interpretation of the references to colour in this figure legend, the reader is referred to the web version of this article.)

under prolonged stress through both a SG-dependent and a SG-independent mechanism and that this pathway is strongly influenced by the ALS-associated genetic background and is different in non-neuronal *versus* neuronal cells. In line with our observations, two recent studies, by using different experimental approaches, showed that the formation of phosphorylated and ubiquitinated TDP-43 granules occurred independently from SG (Gasset-Rosa et al., 2019; Mann et al., 2019). However, they also suggest that the pathological TDP-43 granules may evolve through SG intermediates with TDP-43 protein inside SG remaining within liquid-like RNA-rich droplets in a dynamic state and cytoplasmic TDP-43 passing from liquid droplets into gel/solid-like structures (Gasset-Rosa et al., 2019; Mann et al., 2019).

We also observed that TDP-43 recruited into SG after a prolonged stress is not phosphorylated, suggesting that TDP-43 is protected by phosphorylation when it is recruited within SG, as previously hypothesized (Mann et al., 2019; McGurk et al., 2018). However, when the stress persists becoming chronic as in neurodegeneration, cytoplasmic TDP-43 protein may be in part released from SG and undergo phosphorylation by protein kinases, such as CK1ε through the GADD34/CK1ε complex (Goh et al., 2018), driving a pathological aggregate transition. Altogether, although all the current findings on the mechanistic link between SG and TDP-43 protein aggregation need further validation, they may help in part explain why several studies failed to identify SG markers in pathological TDP-43 inclusions present in post-mortem ALS/FTD brain tissues (Bentmann et al., 2012; Colombrita et al., 2009; McGurk et al., 2014).

In this context, our data also show that SG and P-TDP-43 aggregates are able to dissolve during recovery from our prolonged stress, but we can speculate that during the neurodegenerative process a critical stress threshold exists over which disassembly of SG and P-TDP-43 inclusions becomes an irreversible process, causing the engulfment of the protein quality control system, including chaperones and the autophagic and ubiquitin/proteasome systems. Interestingly, together with SG and P-TDP-43 aggregate formation, we observed p62 accumulation in a very high percentage of cells in both control and mutant fibroblasts and iPSC-MN, suggesting that prolonged oxidative stress impairs autophagy and the ability of SG to properly disassemble (Bjørkøy et al., 2009). According to this, it was shown that, when autophagy is impaired, SG disassembly is also affected because of the accumulation of misfolded proteins (Ganassi et al., 2016), producing insoluble aggregates that disrupt neuronal homeostasis and promote ALS pathogenesis and neurodegeneration (Monahan et al., 2016). While we observed that SG and P-TDP-43-positive aggregates completely dissolved in fibroblasts at 72-h recovery from prolonged ARS stress, smaller p62 aggregates still persisted, confirming that a defective autophagy system may gradually contribute to an impairment of the protein quality control. We found that chronic ARS treatment increased the number of p62-TIAR- and LC3-TIAR-positive autophagic vacuoles, reinforcing the idea that p62, through autophagy, plays a direct and pivotal role in efficient SG clearance.

These data are consistent with a different cell response to stress shown by mC9ORF72 fibroblasts in view of the fact that C9ORF72 protein is a regulator of endosomal and vesicular trafficking and is directly involved in regulating autophagy (Farg et al., 2014). Remarkably, it has been demonstrated that C9ORF72 colocalizes with Ubiquilin-2 and LC3-positive vesicles (Leskelä et al., 2019) and we found a lower amount of TIAR/LC3 vacuoles in mC9ORF72 fibroblasts. Additionally, C9ORF72 protein was recently described to form a complex with the autophagy receptor p62, which associates with symmetrically methylated arginine proteins enriched in SG, controlling SG removal by autophagy (Chitiprolu et al., 2018). Therefore, all these data, together with the present findings, suggest that an impairment of the p62-dependent clearance of SG components may be amplified in ALS patients with *C9ORF72* repeat expansions, due to the haploinsufficiency of C9ORF72 protein observed in such patients (Haeusler et al., 2016).

5. Conclusions

Here we provide evidence that also a mild and prolonged oxidative stress in human primary fibroblasts and iPSC-MN induces the formation of SG in association to the appearance of distinct P-TDP-43 cytoplasmic inclusions, with differences in stress response depending on cell type and genetic background. Therefore, ALS patient-derived cells, exposed to a persistent oxidative stress, may represent a suitable bioassay to study not only TDP-43 pathology, but also to test potential drugs able to prevent or disaggregate P-TDP-43 inclusions. Most of the cellular and animal models used so far have indeed failed to fully reproduce ALS/FTD pathology, while our results sustain the translatability of common pathomechanisms from patient-derived peripheral cell models, such as fibroblasts, to human differentiated iPSC-MN, opening the scenario of new therapeutic approaches also for individual rehabilitation of patients.

Ethics approval and consent to participate

Skin biopsies of healthy individuals and patients were obtained after written informed consent and in accordance with guidelines approved by the local ethics committee (IRCCS Istituto Auxologico Italiano Review Board).

Consent for publication

Not applicable.

Availability of data and material

Not applicable.

Competing interests

The authors declare that they have no competing interests.

Funding

Financial support was received by Fondazione Regionale per la Ricerca Biomedica (Regione Lombardia), Project nr. 2015–0023. AR was granted by the Italian Ministry of Education, University and

Research (MIUR, PRIN2015 Call). DB was supported by a fellowship of "Aldo Ravelli" Center for Neurotechnology and Experimental Brain Therapeutics, Università degli Studi di Milano.

Acknowledgments

Special thanks to the patients because without their generous contribution this study would not have been possible.

We also thank the Cell line and DNA bank of pediatric movement disorders and mitochondrial diseases of the Telethon Network of Genetic Biobanks (Project GTB07001) for donation of one healthy fibroblast cell line. All authors read and approved the final manuscript.

Appendix A. Supplementary data

Supplementary data to this article can be found online at https://doi.org/10.1016/j.nbd.2020.105051.

References

Abramzon, Y.A., Fratta, P., Traynor, B.J., Chia, R., 2020. The overlapping genetics of amyotrophic lateral sclerosis and frontotemporal dementia. Front. Neurosci. https://doi.org/10.3389/fnins.2020.00042.

Anderson, P.K.N., 2009. Stress granules. Curr. Biol. 19 (10), R397–R398. https://doi.org/10.1016/j.cub.2009.03.013.

Arai, T., Hasegawa, M., Akiyama, H., Ikeda, K., Nonaka, T., Mori, H., Mann, D., Tsuchiya, K., Yoshida, M., Hashizume, Y., Oda, T., 2006. TDP-43 is a component of ubiquitin-positive tau-negative inclusions in frontotemporal lobar degeneration and amyotrophic lateral sclerosis. Biochem. Biophys. Res. Commun. 351, 602–611. https://doi.org/10.1016/j.bbrc.2006.10.093.

Aulas, A., Velde, C.V., 2015. Alterations in stress granule dynamics driven by TDP-43 and FUS: A link to pathological inclusions in ALS? Front. Cell. Neurosci. 9, 423. https://doi.org/10.3389/fncel.2015.00423.

Aulas, A., Caron, G., Gkogkas, C.G., Mohamed, N.V., Destroismaisons, L., Sonenberg, N., Leclerc, N., Alex Parker, J., Velde, C. Vande, 2015. G3BP1 promotes stress-induced RNA granule interactions to preserve polyadenylated mRNA. J. Cell Biol. https://doi.org/10.1083/jcb.201408092.

Bardelli, D., Sassone, F., Colombrita, C., Volpe, C., Gumina, V., Peverelli, S., Catusi, I., Ratti, A., Silani, V., Bossolasco, P., 2020. Reprogramming fibroblasts and peripheral blood cells from a C9ORF72 patient: a proof-of-principle study. J. Cell. Mol. Med. https://doi.org/10.1111/jcmm.15048.

Bentmann, E., Neumann, M., Tahirovic, S., Rodde, R., Dormann, D., Haass, C., 2012. Requirements for stress granule recruitment of fused in sarcoma (FUS) and TAR DNA-binding protein of 43 kDa (TDP-43). J. Biol. Chem. 287, 23079–23094. https://doi.org/10.1074/jbc.M111.328757.

Birsa, N., Bentham, M.P., Fratta, P., 2019. Cytoplasmic functions of TDP-43 and FUS and their role in ALS. Semin. Cell Dev. Biol. https://doi.org/10.1016/j.semcdb.2019.05.023.

Bjørkøy, G., Lamark, T., Pankiv, S., Øvervatn, A., Brech, A., Johansen, T., 2009. Monitoring autophagic degradation of p62/SQSTM1. Methods Enzymol. 452, 181–197. https://doi.org/10.1016/S0076-6879(08)03612-4.

Bosco, D.A., Lemay, N., Ko, H.K., Zhou, H., Burke, C., Kwiatkowski, T.J., Sapp, P., Mckenna-Yasek, D., Brown, R.H., Hayward, L.J., 2010. Mutant FUS proteins that cause amyotrophic lateral sclerosis incorporate into stress granules. Hum. Mol. Genet 19 (21), 4160–4175. https://doi.org/10.1093/hmg/ddq335.

Bossolasco, P., Sassone, F., Gumina, V., Peverelli, S., Garzo, M., Silani, V., 2018. Motor neuron differentiation of iPSCs obtained from peripheral blood of a mutant TARDBP ALS patient. Stem Cell Res. 30, 61–68. https://doi.org/10.1016/j.scr.2018.05.009.

Cascella, R., Fani, G., Capitini, C., Rusmini, P., Poletti, A., Cecchi, C., Chiti, F., 2017. Quantitative assessment of the degradation of aggregated TDP-43 mediated by the ubiquitin proteasome system and macroautophagy. FASEB J. 31 (12), 5609–5624. https://doi.org/10.1096/fj.201700292RR.

Chitiprolu, M., Jagow, C., Tremblay, V., Bondy-Chorney, E., Paris, G., Savard, A., Palidwor, G., Barry, F.A., Zinman, L., Keith, J., Rogaeva, E., Robertson, J., Lavallée-Adam, M., Woulfe, J., Couture, J.F., Côté, J., Gibbings, D., 2018. A complex of C9ORF72 and p62 uses arginine methylation to eliminate stress granules by autophagy. Nat. Commun. 9 (1), 2794. https://doi.org/10.1038/s41467-018-05273-7.

Colombrita, C., Zennaro, E., Fallini, C., Weber, M., Sommacal, A., Buratti, E., Silani, V., Ratti, A., 2009. TDP-43 is recruited to stress granules in conditions of oxidative insult. J. Neurochem. 111, 1051–1061. https://doi.org/10.1111/j.1471-4159.2009.06383.x.

Daigle, G.G., Lanson, N.A., Smith, R.B., Casci, I., Maltare, A., Monaghan, J., Nichols, C.D., Kryndushkin, D., Shewmaker, F., Pandey, U.B., 2013. Rna-binding ability of FUS regulates neurodegeneration, cytoplasmic mislocalization and incorporation into stress granules associated with FUS carrying ALS-linked mutations. Hum. Mol. Genet. 22 (6), 1193–1205. https://doi.org/10.1093/hmg/dds526.

Dormann, D., Rodde, R., Edbauer, D., Bentmann, E., Fischer, I., Hruscha, A., Than, M.E., MacKenzie, I.R.A., Capell, A., Schmid, B., Neumann, M., Haass, C., 2010. ALS-associated fused in sarcoma (FUS) mutations disrupt transportin-mediated nuclear import. EMBO J. 29 (16), 2841–2857. https://doi.org/10.1038/emboj.2010.143.

Dunn, K.W., Kamocka, M.M., McDonald, J.H., 2011. A practical guide to evaluating colocalization in biological microscopy. Am. J. Physiol. - Cell Physiol. https://doi.org/10.1152/ajpcell.00462.2010.

Fang, M.Y., Markmiller, S., Vu, A.Q., Javaherian, A., Dowdle, W.E., Jolivet, P., Bushway, P.J., Castello, N.A., Baral, A., Chan, M.Y., Linsley, J.W., Linsley, D., Mercola, M., Finkbeiner, S., Lecuyer, E., Lewcock, J.W., Yeo, G.W., 2019. Small-molecule modulation of TDP-43 recruitment to stress granules prevents persistent TDP-43 accumulation in ALS/FTD. Neuron 103 (5), 802–819.e11. https://doi.org/10.1016/j.neuron.2019.05.048.

Farg, M.A., Sundaramoorthy, V., Sultana, J.M., Yang, S., Atkinson, R.A.K., Levina, V., Halloran, M.A., Gleeson, P.A., Blair, I.P., Soo, K.Y., King, A.E., Atkin, J.D., 2014. C9ORF72, implicated in amytrophic lateral sclerosis and frontotemporal dementia, regulates endosomal trafficking. Hum. Mol. Genet. 23 (13), 3579–3595. https://doi.org/10.1093/hmg/ddu068.

Ganassi, M., Mateju, D., Bigi, I., Mediani, L., Poser, I., Lee, H.O., Seguin, S.J., Morelli, F.F., Vinet, J., Leo, G., Pansarasa, O., Cereda, C., Poletti, A., Alberti, S., Carra, S., 2016. A surveillance function of the HSPB8-BAG3-HSP70 chaperone complex ensures stress granule integrity and dynamism. Mol. Cell 63 (5), 796–810. https://doi.org/10.1016/j.molcel.2016.07.021.

Gasset-Rosa, F., Lu, S., Yu, H., Chen, C., Melamed, Z., Guo, L., Shorter, J., Da Cruz, S., Cleveland, D.W., 2019. Cytoplasmic TDP-43 De-mixing independent of stress granules drives inhibition of nuclear import, loss of nuclear TDP-43, and cell death. Neuron 102, 339–357.e7. https://doi.org/10.1016/j.neuron.2019.02.038.

Gilks, N., Kedersha, N., Ayodele, M., Shen, L., Stoecklin, G., Dember, L.M., Anderson, P., 2004. Stress granule assembly is mediated by prion-like aggregation of TIA-1. Mol. Biol. Cell 15 (12), 5383–5398. https://doi.org/10.1091/mbc.E04-08-0715.

Goh, C.W., Lee, I.C., Sundaram, J.R., George, S.E., Yusoff, P., Brush, M.H., Sze, N.S.K., Shenolikar, S., 2018. Chronic oxidative stress promotes GADD34-mediated phosphorylation of the TAR DNA-binding protein TDP-43, a modification linked to neurodegeneration. J. Biol. Chem. 293 (1), 163–176. https://doi.org/10.1074/jbc.M117.814111.

Gopal, P.P., Nirschl, J.J., Klinman, E., Holzbaurb, E.L.F., 2017. Amyotrophic lateral sclerosis-linked mutations increase the viscosity of liquid-like TDP-43 RNP granules in neurons. Proc. Natl. Acad. Sci. U. S. A 114, E2466–E2475. https://doi.org/10.1073/pnas.1614462114.

Haeusler, A.R., Donnelly, C.J., Rothstein, J.D., 2016. The expanding biology of the C9orf72 nucleotide repeat expansion in neurodegenerative disease. Nat. Rev. Neurosci. https://doi.org/10.1038/nrn.2016.38.

Harrison, A.F., Shorter, J., 2017. RNA-binding proteins with prion-like domains in health and disease. Biochem. J. https://doi.org/10.1042/BCJ20160499.

Hyman, A.A., Weber, C.A., Jülicher, F., 2014. Liquid-liquid phase separation in biology. Annu. Rev. Cell Dev. Biol. 30, 39–58. https://doi.org/10.1146/annurev-cellbio-100913-013325.

Johnson, B.S., Snead, D., Lee, J.J., McCaffery, J.M., Shorter, J., Gitler, A.D., 2009. TDP-43 is intrinsically aggregation-prone, and amyotrophic lateral sclerosis-linked mutations accelerate aggregation and increase toxicity. J. Biol. Chem. 284 (30), 20329–20339. https://doi.org/10.1074/jbc.M109.010264.

Kedersha, N., Anderson, P., 2002. Stress granules: Sites of mRNA triage that regulate mRNA stability and translatability. Biochem. Soc. Trans. 30 (Pt 6), 963–969. https://doi.org/10.1042/BST0300963.

Lenzi, J., De Santis, R., De Turris, V., Morlando, M., Laneve, P., Calvo, A., Caliendo, V., Chiò, A., Rosa, A., Bozzoni, I., 2015. ALS mutant FUS proteins are recruited into stress granules in induced pluripotent stem cell-derived motoneurons. DMM Dis. Model. Mech. 8 (7), 755–766. https://doi.org/10.1242/dmm.020099.

Lenzi, P., Lazzeri, G., Biagioni, F., Busceti, C.L., Gambardella, S., Salvetti, A., Fornai, F., 2016. The autophagoproteasome a novel cell clearing organelle in baseline and stimulated conditions. Front. Neuroanat. 10, 78. https://doi.org/10.3389/fnana.2016.00078.

Leskelä, H., Rostalski, N., Remes, T., Hiltunen, H., 2019. C9orf72 proteins regulate autophagy and undergo autophagosomal or proteasomal degradation in a cell type-dependent manner. Cells. https://doi.org/10.3390/cells8101233.

Ling, S.C., Polymenidou, M., Cleveland, D.W., 2013. Converging mechanisms in als and FTD: Disrupted RNA and protein homeostasis. Neuron. https://doi.org/10.1016/j.neuron.2013.07.033.

Liu-Yesucevitz, L., Bilgutay, A., Zhang, Y.J., Vanderwyde, T., Citro, A., Mehta, T., Zaarur, N., McKee, A., Bowser, R., Sherman, M., Petrucelli, L., Wolozin, B., 2010. Tar DNA binding protein-43 (TDP-43) associates with stress granules: Analysis of cultured cells and pathological brain tissue. PLoS One 5 (10), e13250. https://doi.org/10.1371/journal.pone.0013250.

Mahboubi, H., Stochaj, U., 2017. Cytoplasmic stress granules: Dynamic modulators of cell signaling and disease. Biochim. Biophys. Acta - Mol. Basis Dis. https://doi.org/10.1016/j.bbadis.2016.12.022.

Mann, J.R., Gleixner, A.M., Mauna, J.C., Gomes, E., DeChellis-Marks, M.R., Needham, P.G., Copley, K.E., Hurtle, B., Portz, B., Pyles, N.J., Guo, L., Calder, C.B., Wills, Z.P., Pandey, U.B., Kofler, J.K., Brodsky, J.L., Thathiah, A., Shorter, J., Donnelly, C.J., 2019. RNA binding antagonizes neurotoxic phase transitions of TDP-43. Neuron 102, 321–338.e8. https://doi.org/10.1016/j.neuron.2019.01.048.

McGurk, L., Lee, V.M., Trojanowksi, J.Q., Van Deerlin, V.M., Lee, E.B., Bonini, N.M., 2014. Poly-A binding protein-1 localization to a subset of TDP-43 inclusions in amyotrophic lateral sclerosis occurs more frequently in patients harboring an expansion in C9orf72. J. Neuropathol. Exp. Neurol. 73 (9), 837–845. https://doi.org/10.1097/NEN.0000000000000102.

McGurk, L., Gomes, E., Guo, L., Mojsilovic-Petrovic, J., Tran, V., Kalb, R.G., Shorter, J., Bonini, N.M., 2018. Poly(ADP-ribose) prevents pathological phase separation of TDP-43 by promoting liquid demixing and stress granule localization. Mol. Cell 71 (5), 703–717.e9. https://doi.org/10.1016/j.molcel.2018.07.002.

Molliex, A., Temirov, J., Lee, J., Coughlin, M., Kanagaraj, A.P., Kim, H.J., Mittag, T., Taylor, J.P., 2015. Phase separation by low complexity domains promotes stress granule assembly and drives pathological fibrillization. Cell 163, 123–133. https://doi.org/10.1016/j.cell.2015.09.015.

Monahan, Z., Shewmaker, F., Pandey, U.B., 2016. Stress granules at the intersection of autophagy and ALS. Brain Res. https://doi.org/10.1016/j.brainres.2016.05.022.

Neumann, M., Sampathu, D.M., Kwong, L.K., Truax, A.C., Micsenyi, M.C., Chou, T.T., Bruce, J., Schuck, T., Grossman, M., Clark, C.M., McCluskey, L.F., Miller, B.L., Masliah, E., Mackenzie, I.R., Feldman, H., Feiden, W., Kretzschmar, H.A., Trojanowski, J.Q., Lee, V.M.Y., 2006. Ubiquitinated TDP-43 in frontotemporal lobar degeneration and amyotrophic lateral sclerosis. Science (80) 314 (5796), 130–133. https://doi.org/10.1126/science.1134108.

Neumann, M., Kwong, L.K., Lee, E.B., Kremmer, E., Flatley, A., Xu, Y., Forman, M.S., Troost, D., Kretzschmar, H.A., Trojanowski, J.Q., Lee, V.M.Y., 2009. Phosphorylation of S409/410 of TDP-43 is a consistent feature in all sporadic and familial forms of TDP-43 proteinopathies. Acta Neuropathol. 117 (2), 137–149. https://doi.org/10.1007/s00401-008-0477-9.

Onesto, E., Colombrita, C., Gumina, V., Borghi, M.O., Dusi, S., Doretti, A., Fagiolari, G., Invernizzi, F., Moggio, M., Tiranti, V., Silani, V., Ratti, A., 2016. Gene-specific mitochondria dysfunctions in human TARDBP and C9ORF72 fibroblasts. Acta Neuropathol. Commun. 4 (1), 47. https://doi.org/10.1186/s40478-016-0316-5.

Orrù, S., Coni, P., Floris, A., Littera, R., Carcassi, C., Sogos, V., Brancia, C., 2016. Reduced stress granule formation and cell death in fibroblasts with the A382T mutation of TARDBP gene: evidence for loss of TDP-43 nuclear function. Hum. Mol. Genet. 25 (20), 4473–4483. https://doi.org/10.1093/hmg/ddw276.

Ratti, A., Buratti, E., 2016. Physiological functions and pathobiology of TDP-43 and FUS/TLS proteins. J. Neurochem. https://doi.org/10.1111/jnc.13625.

Ross Buchan, J., Nissan, T., Parker, R., 2010. Analyzing P-bodies and stress granules in *Saccharomyces cerevisiae*. Methods Enzymol. 470, 619–640. https://doi.org/10.1016/S0076-6879(10)70025-2.

Schmidt, H.B., Rohatgi, R., 2016. In vivo formation of vacuolated multi-phase compartments lacking membranes. Cell Rep. 16 (5), 1228–1236. https://doi.org/10.1016/j.celrep.2016.06.088.

Swanlund, J.M., Kregel, K.C., Oberley, T.D., 2010. Investigating autophagy: quantitative morphometric analysis using electron microscopy. Autophagy 6 (2), 270–277. https://doi.org/10.4161/auto.6.2.10439.

Volkening, K., Leystra-Lantz, C., Yang, W., Jaffee, H., Strong, M.J., 2009. Tar DNA binding protein of 43 kDa (TDP-43), 14-3-3 proteins and copper/zinc superoxide dismutase (SOD1) interact to modulate NFL mRNA stability. Implications for altered RNA processing in amyotrophic lateral sclerosis (ALS). Brain Res. 130, 168–182. https://doi.org/10.1016/j.brainres.2009.09.105.

Wang, M., Wang, H., Tao, Z., Xia, Q., Hao, Z., Prehn, J.H.M., Zhen, X., Wang, G., Ying, Z., 2020. C9orf72 associates with inactive Rag GTPases and regulates mTORC1-mediated autophagosomal and lysosomal biogenesis. Aging Cell. https://doi.org/10.1111/acel.13126.

Webster, C.P., Smith, E.F., Bauer, C.S., Moller, A., Hautbergue, G.M., Ferraiuolo, L., Myszczynska, M.A., Higginbottom, A., Walsh, M.J., Whitworth, A.J., Kaspar, B.K., Meyer, K., Shaw, P.J., Grierson, A.J., De Vos, K.J., 2016. The C9orf72 protein interacts with Rab1a and the ULK 1 complex to regulate initiation of autophagy. EMBO J. 35 (15), 1656–1676. https://doi.org/10.15252/embj.201694401.

Wheeler, J.R., Matheny, T., Jain, S., Abrisch, R., Parker, R., 2016. Distinct stages in stress granule assembly and disassembly. Elife 5, e18413. https://doi.org/10.7554/eLife.18413. pii.

Wippich, F., Bodenmiller, B., Trajkovska, M.G., Wanka, S., Aebersold, R., Pelkmans, L., 2013. Dual specificity kinase DYRK3 couples stress granule condensation/dissolution to mTORC1 signaling. Cell 152 (4), 791–805. https://doi.org/10.1016/j.cell.2013.01.033.